

Review

# Prospects of Synthesized Magnetic TiO<sub>2</sub>-Based Membranes for Wastewater Treatment: A Review

E. Kweinor Tetteh <sup>\*</sup>, S. Rathilal , D. Asante-Sackey  and M. Noro Chollom

Green Engineering and Sustainability Research Group, Department of Chemical Engineering, Faculty of Engineering and the Built Environment, Steve Biko Campus, Durban University of Technology, Durban 4001, South Africa; rathilals@dut.ac.za (S.R.); ingsackey@gmail.com (D.A.-S.); mnchollom@gmail.com (M.N.C.)

\* Correspondence: emmanuelk@dut.ac.za or ektetteh34@gmail.com

**Abstract:** Global accessibility to clean water has stressed the need to develop advanced technologies for the removal of toxic organic and inorganic pollutants and pathogens from wastewater to meet stringent discharge water quality limits. Conventionally, the high separation efficiencies, relative low costs, small footprint, and ease of operation associated with integrated photocatalytic-membrane (IPM) technologies are gaining an all-inclusive attention. Conversely, photocatalysis and membrane technologies face some degree of setbacks, which limit their worldwide application in wastewater settings for the treatment of emerging contaminants. Therefore, this review elucidated titanium dioxide (TiO<sub>2</sub>), based on its unique properties (low cost, non-toxicity, biocompatibility, and high chemical stability), to have great potential in engineering photocatalytic-based membranes for reclamation of wastewater for re-use. The environmental pathway of TiO<sub>2</sub> nanoparticles, membranes and configuration types, modification process, characteristics, and applications of IPMs in water settings are discussed. Future research and prospects of magnetized TiO<sub>2</sub>-based membrane technology is highlighted as a viable water purification technology to mitigate fouling in the membrane process and photocatalyst recoverability. In addition, exploring life cycle assessment research would also aid in utilizing the concept and pressing for large-scale application of this technology.

**Keywords:** advanced oxidation process; titanium dioxide (TiO<sub>2</sub>); photocatalysis; magnetic TiO<sub>2</sub>; membranes; wastewater treatment



**Citation:** Tetteh, E.K.; Rathilal, S.; Asante-Sackey, D.; Chollom, M.N. Prospects of Synthesized Magnetic TiO<sub>2</sub>-Based Membranes for Wastewater Treatment: A Review. *Materials* **2021**, *14*, 3524. <https://doi.org/10.3390/ma14133524>

Academic Editor: Elisabete Maria Dos Santos Castanheira Coutinho

Received: 9 May 2021  
Accepted: 14 June 2021  
Published: 24 June 2021

**Publisher's Note:** MDPI stays neutral with regard to jurisdictional claims in published maps and institutional affiliations.



**Copyright:** © 2021 by the authors. Licensee MDPI, Basel, Switzerland. This article is an open access article distributed under the terms and conditions of the Creative Commons Attribution (CC BY) license (<https://creativecommons.org/licenses/by/4.0/>).

## 1. Introduction

In a growing economy, clean and drinkable water, free from toxic chemicals, carcinogenic substances and harmful microorganisms are essential for human health and sustainability [1,2]. However, the fast population growth associated with urbanization, irrigated agriculture and industrialization have driven the environmental concern of wastewater and demand for fresh water globally [3,4]. This opioid epidemic, be it due to insufficient accessibility to clean water, poor water quality or waterborne diseases, has seriously threatened human lives in many underdeveloped and developing countries [4–6]. The result has been an upsurge of stringent environmental standards to provide clean water with high quality and sustainable waste management facilities [4–7]. In addition, conventional technologies (coagulation, flocculation, biological) are limited when it comes to complete decontamination of water containing emerging contaminants (hormones, persistent organic pollutants, antibiotics, pharmaceuticals, heavy metals, nano plastics, etc.) [6,8–10], and to avoid secondary pollution problems an advanced treatment technology is required. It is therefore valuable to explore the development of advanced wastewater treatment technologies to effectively purify water in a more ecofriendly and economical routine.

In recent years, advances in nanoengineering and nanotechnology to develop nanosorbents, nanocatalysts, bioactive nanoparticles, and filtration systems coupled with nanoparticles have been seen to be very promising in wastewater treatment settings [1,9,11–15].

Most of the nanotechnology-based materials can exhibit distinctive physical and chemical properties at a nanoscale (1–100 nm) as compared to their bulk complements [9,12]. Intensive research devoted to understanding the fundamental mechanism of nano-based materials has revealed that semiconductor photocatalysts, such as TiO<sub>2</sub>, possess high surface-to-volume ratios, chemical stability, hydrophilicity and high photo-reactivity with antireflection and self-cleaning abilities [13,16,17]. Semiconductor photocatalysis is driven by energy sources (UV light, ultrasonic, heat or sunlight) to activate metal oxides (TiO<sub>2</sub>, ZnO, and Fenton reagent) in order to generate radical species (OH<sup>−</sup>, H<sup>+</sup>) in the occurrence of wet or air oxidation states like ozone or hydrogen peroxide [10,18–21].

Heterogeneous photocatalysts and semiconductors assisted with UV light for photodegradation of organic pollutants in water and wastewater settings have been reported by many researchers [9,11,16,22,23]. These include BiVO<sub>4</sub>, TiO<sub>2</sub> Fe–ZnIn<sub>2</sub>S<sub>4</sub>, WO<sub>3</sub>, BiOBr, BiFeO<sub>3</sub>, Fe<sub>2</sub>O<sub>3</sub>, CuS, and ZnO [11,17,24]. Among these photocatalysts and nanoparticles, titanium dioxide (TiO<sub>2</sub>), being cheap, commercially available, nontoxic and chemically stable, has been the most extensively researched in water settings [25–27]. Aside from water and wastewater treatment applications, the TiO<sub>2</sub> photocatalyst has been widely used in air purification and other biological applications [25,28–33]. Notwithstanding, there are several setbacks associated with TiO<sub>2</sub> industrial applications at a large scale via the advanced oxidation process (AOP) [11,18,25,34,35]. Some of these include high cost of energy resources and chemicals as oxidants and their potential to handle large amounts of wastewater with high organic strengths [11,34,35]. The separation, recovery, and re-use of TiO<sub>2</sub> nanoparticles is also a major constraint to its industrial applications [34,36,37].

In general, most chemicals or nanoparticles used in conventional systems end up converting contaminants from one form to another [11,15]. For instance, generation of biosolids or sludge becomes the new pollutant, which requires further treatment before discharge. Additionally, in the application of TiO<sub>2</sub> photocatalysis, the low rate of electrostatic interaction to oxygen and high rate of electron-hole recombination significantly slows its adsorption of organic contaminants onto its surface [11,38]. Yet, there are still some research gaps associated with TiO<sub>2</sub> nanoparticle applications, which include low quantum efficiency due to inefficient visible light harvesting, acceptable photoreactor design, recovery, re-use, scale-up, etc. [25]. Thus, in conjunction with unaddressed concerns of emerging contaminants [1], the search for ecofriendly techniques capable of degrading pollutants rather than simply converting them from one form to another becomes essential. Consequentially, many researchers have pursued to develop new heterogeneous photocatalysts with a suitable crystal structure, high specific surface area, and easy separation and re-use capabilities [18,26,30,39]. This includes synthesizing metal/TiO<sub>2</sub> nanocomposites as an efficient way to improve TiO<sub>2</sub> photocatalytic efficiency by enhancing its electron-hole separation [18,30,40]. In addition, the embedding of Fe<sub>3</sub>O<sub>4</sub> has been proven to be very useful in order to provide TiO<sub>2</sub> with magnetic separation ability [41–43].

#### *Research Approach*

Conventionally, post-treatment of wastewater with membrane filtration or TiO<sub>2</sub> immobilization via AOP has been applied and reported by many researchers. These processes, however, face problems such as membrane fouling and loss of effective catalysts [30,44,45]. Although substantial progress has been made in developing membrane technologies at a large scale, much work is expected for TiO<sub>2</sub> photocatalysis to become a commercialized technology in wastewater treatment settings. Therefore, in this review the basics of photocatalysis are discussed with TiO<sub>2</sub> nanoparticles and recombination with membrane technology as well as the mechanisms involved to prioritize their usage in the water and wastewater treatment sector [46–48]. This was carried out via a desktop approach, where a search of literature with keywords such as membrane, TiO<sub>2</sub> photocatalyst, advanced oxidation process (AOP) and integrated photocatalytic membrane (IPM) was conducted utilizing Google scholar, Web of Science, PubMed, and the ScienceDirect database, as shown in Figure 1. The data obtained from 2011–2021 were refined based on the following categories: subscribed journals, article type, publication title, subject area and access type

(open access or achieve). Even though the progression of membrane technology (Figure 1a) as of 20 April 2021 seems to be low (<60,000), its publication supersedes AOP (Figure 1b; <25,000), followed by IPM (Figure 1c; <2500), and then TiO<sub>2</sub> photocatalysis (Figure 1d; <1000). Apparently, the knowledge of IPM is still limited and therefore should be given attention.

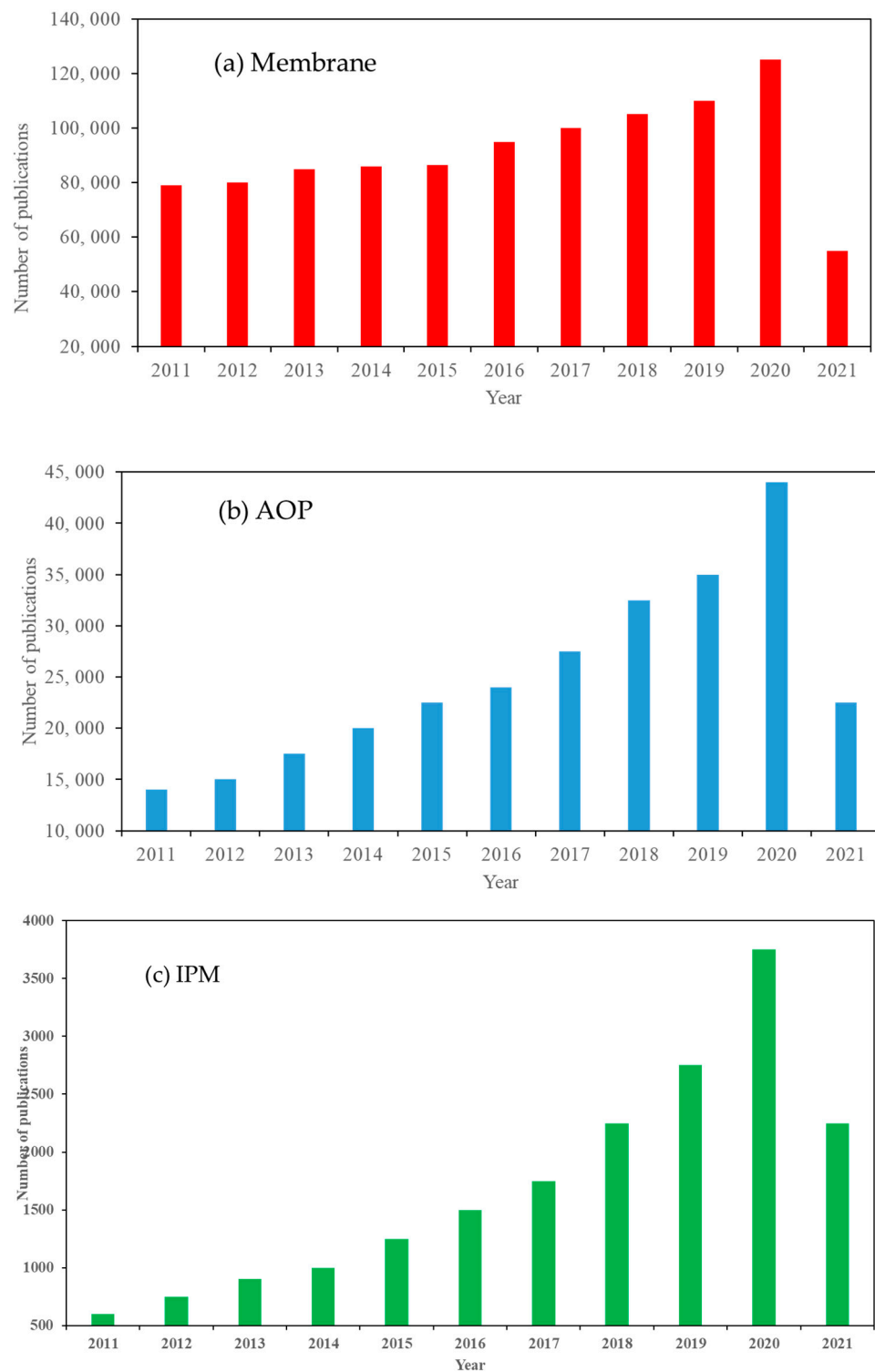
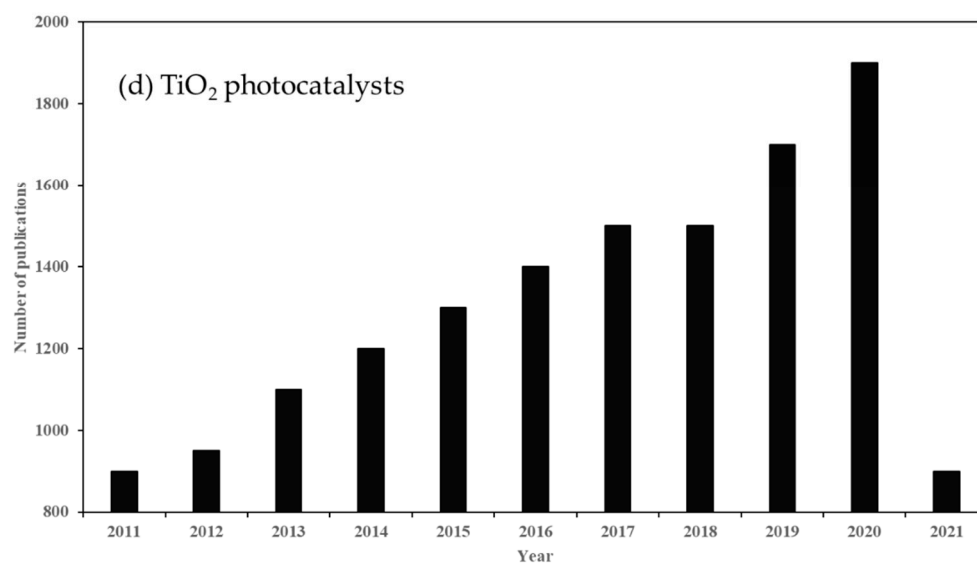


Figure 1. Cont.



**Figure 1.** Publication trend of (a) membranes, (b) advanced oxidation processes (AOP), (c) integrated photocatalytic processes (IPM), and (d) TiO<sub>2</sub> photocatalysts, from 2011–2021 (Web of Science database, 20 April 2021).

## 2. Advanced Oxidation Process (AOP)

Advanced oxidation processes (AOPs) have attracted a great deal of attention of stakeholders in the water and wastewater treatment sector. Photocatalytic degradation technology, being one of the AOPs, involves the use of a semiconductor photocatalyst and photogeneration of highly oxidative hydroxyl radicals [22,34]. In addition, the chemical reactions in AOPs caused by the absorption or desorption of photocatalysts remains unchanged in both photocatalysis and photoelectrochemical splitting of water using titanium [19,22,49]. Furthermore, AOPs differ from conventional chemical and biological wastewater treatment systems as their produced hydroxyl radicals are potent oxidants used to degrade toxic and recalcitrant contaminants into simple and harmless inorganic molecules without creating a secondary excess [46,50,51]. Additionally, AOPs are very robust so as to enhance precipitations and elimination of heavy metals as metal hydroxides, and subsequently, based on the irradiation period, can lead to total mineralization [19,34,52]. AOPs are classified into two categories, namely homogeneous and heterogeneous systems, that can be carried out with or without UV radiation. Table 1 presents some of the reported AOPs commonly used in wastewater treatment settings. The thermal Fenton reaction process is a homogeneous process that involves Fe<sup>2+</sup> reacting with H<sub>2</sub>O<sub>2</sub>. The aforementioned phase (Fe<sup>2+</sup>/Fe<sup>3+</sup>, H<sub>2</sub>O<sub>2</sub>, UV-Vis) is commonly termed as a photo-Fenton reaction [19]. Heterogeneous photocatalysis involves a photoinduced reaction accelerated by the presence of TiO<sub>2</sub> photocatalysts [53,54]. This process stands out among the heterogeneous AOPs because UV irradiation of TiO<sub>2</sub> creates hydroxyl radicals. This facilitates the oxidation and more efficient mineralization of organic material present in the effluent when it is photocatalyzed [55]. In contrast with other AOPs and biological treatments, TiO<sub>2</sub> photocatalysis offers significant advantages [19,46]. Thus, the TiO<sub>2</sub>/UV system can handle contaminants in both the gas and solution phases. Furthermore, TiO<sub>2</sub> is inexpensive, practically insoluble in water, and biologically and chemically inert [19,22,46].

**Table 1.** Types of advanced oxidation processes; adapted from [19,46].

Chemical Process	Photochemical Process
Wet air oxidation	Photo-Fenton reaction
Supercritical water oxidation	UV/ultrasound system
Ultrasound/H <sub>2</sub> O <sub>2</sub> system	UV/O <sub>3</sub> /H <sub>2</sub> O <sub>2</sub> system
Ultrasound/Sonolysis	UV/H <sub>2</sub> O <sub>2</sub> system
Fenton reaction	UV/O <sub>3</sub> system
Ozonation in alkaline	UV photolysis
O <sub>3</sub> /H <sub>2</sub> O <sub>2</sub> system	UV/O <sub>2</sub> /TiO <sub>2</sub> system
Electron—Fenton reaction	UV/H <sub>2</sub> O <sub>2</sub> /TiO <sub>2</sub> system

### 2.1. TiO<sub>2</sub> Photocatalyst

TiO<sub>2</sub> is the most widely used photocatalyst because of its strong physical and chemical stability, insolubility in water, resistance to acids, inertness to most chemicals and long-term photostability [25,40,47]. TiO<sub>2</sub> exhibits three main crystal structures such as rutile (stable), anatase (metastable), and brookite structures (Table 2).

**Table 2.** Chemo-physical properties of TiO<sub>2</sub> (adapted from [49,54]).

Crystalline Forms	Anatase	Rutile	Brookite
Crystalline structure	Tetragonal	Tetragonal	Rhombohedral
Lattice constants (nm)	a = b = 0.3733 c = 0.9370	a = b = 0.4584 c = 0.2953	a = 0.5436; b = 0.9166 c = 0.5135
Density (g.cm <sup>-3</sup> )	3.83	4.24	4.17
Bravais lattice	Simple, body-centered	Simple, body-centered	Simple
Melting point (°C)	Turning into rutile	1870	Turning into rutile
Boiling point (°C)	2927	-	-
Band gap (eV)	3.2	3.0	-
Refractive index (ng)	2.5688	2.9467	2.809
Standard heat capacity (cp)	55.52	55.60	-
Dielectric constant	55	110–117	78

The tetragonal structure consists of both rutile and anatase, while brookite has a rhombohedral structure [48–50]. In addition to their shape and nanoscale or size, the unique physicochemical properties of TiO<sub>2</sub> crystals are a result of their intrinsic electronic structure and crystal structures [17,25,51]. Anatase has been found to be more active than rutile, but both forms of TiO<sub>2</sub> have been reported to be photoactive. Additionally, a mixture of anatase and rutile for photocatalysis has been found to exhibit synergy due to the photoinduced interfacial electrons of anatase that can be transformed into rutile [27,39].

Rutile and anatase, with 3.0 eV and 3.2 eV band gaps, respectively, are the most common polymorphs of TiO<sub>2</sub> [49,50]. In Figure 2, the large TiO<sub>2</sub> energy band means that higher UV light energy is required to excite electrons to create hydroxyl radicals, which is the key to the photodegradation of contaminants in the presence of oxygen [20,27,52].

The crystalline phase of anatase is desired because of its maximum efficiency under UV irradiation [20]. The photogenerated electrons form superoxide radicals in the rutile conduction band and the holes in the anatase valence band play a significant role in oxidation reactions. In addition, the 3.2 eV anatase band gap (Figure 2) corresponding to the light wavelength of 388 nm means that only UV light will activate TiO<sub>2</sub>. This limits the use of sunlight and greener energy for the activation of TiO<sub>2</sub>, as only around 5% of sunlight is formed by UV radiation. Thus, during the photo activation step, TiO<sub>2</sub> undergoes a rapid recombination of electrons and holes, which then reduces photoactivity. Hence, by doping the TiO<sub>2</sub> with inert supports, the electron–hole recombination and wide band gap can be addressed while increasing the TiO<sub>2</sub> nanoparticle size [20,25].

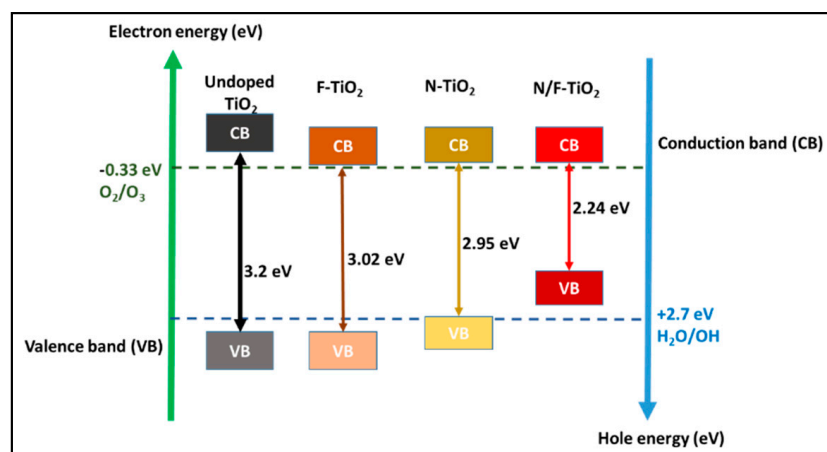


**Figure 2.** Schematic diagram of TiO<sub>2</sub> with different valence and conduction band levels; adapted from [49,53].

Furthermore, in photocatalytic activities, TiO<sub>2</sub> with a valence band (VB) and conduction band (CB) levels of +2.9 and −0.33 eV can result in a band gap energy of 3.2 eV. As shown in Figure 2, the TiO<sub>2</sub> VB and CB levels are more positive and negative than the distinctive redox potential of O<sub>2</sub>/H<sub>2</sub>O (1.23 eV). The presence of Ti<sup>3+</sup> defects beneath the CB surface causes the band gap reduction in F-doped TiO<sub>2</sub> (3.02 eV), while in N-doped TiO<sub>2</sub> (2.95 eV) the mid-band states are created as the N species fill voids as impurities above the VB. However, there is a doping-induced effect and a transition in the VB tail; co-doping N and F into TiO<sub>2</sub> results in the greatest band gap reduction, from 3.2 eV to 2.24 eV (Figure 2).

### 2.1.1. TiO<sub>2</sub> Modification Supports

In wastewater treatment settings, TiO<sub>2</sub> photocatalysis in practical applications is very limited due to low quantum efficiency under visible radiations as well as difficulties of being separated in suspensions [18,55,56]. To ensure that TiO<sub>2</sub> will work optimally without any complexity, modification becomes essential [6,54]. Filtration following photocatalytic activities is very costly and, therefore, catalyst supports can be explored. Some of the supporting materials of TiO<sub>2</sub> reported include glass beads, fiber, glass, silica and zeolite mater [6,20,25,53,57]. Consequently, there are diverse techniques used to modify TiO<sub>2</sub>, where doping of pure TiO<sub>2</sub> with either anions or cations remain one of the most common methods for enhancing its sensitivity to visible light and lowering the rate of charge carrier recombination [20,39,53,54]. Furthermore, photocatalysts synthesized via chemical doping or ion implantation with metals and nonmetals result in a narrowing of the TiO<sub>2</sub> band gap as well as the crystal lattice or structure [20,25,39]. Therefore, in selecting these metals and nonmetals, their sensitivity should be considered.

- Cationic doping of TiO<sub>2</sub>

To dope TiO<sub>2</sub>, cations like rare earth metals, noble metals, weak metals and transition metals have been used [26]. In addition, when a metallic ion is doped with TiO<sub>2</sub>, the light absorption range expands, whereas the redox potential of the photogenerated radicals increases [58–60]. This generally results in the transfer of photoexcited electrons from the TiO<sub>2</sub> conduction band to metal particles deposited on the TiO<sub>2</sub> surface. Cationic doping can also decrease the probability of electron–hole recombination, leading to an effective separation of the charge and thus improved photocatalytic activity [61]. However, the nature and concentration of the dopant inducing the charge surface together with the corrosion mechanism can affect the photocatalytic property of the materials [20,40]. Thus, cationic dopants have a distinctive impact on the catalyst lattice. Some of these metal dopants (Ag, Fe, Mn, Ni, Cu, Pt, Rh, and Pd) act as free electrons, which facilitates the conjugation of the photogenerated carriers [26]. Conversely, metal-doped materials have

been reported to be thermodynamically unstable, which can be captured on the TiO<sub>2</sub> band gap at the d-level and can subsequently shift the redox potential [26,30,62,63]. However, by removing the electron hole, TiO<sub>2</sub> doped with metallic cations with lower oxidation states can maintain electron stability [30]. In addition, TiO<sub>2</sub> doped with metallic cations with higher oxidation states, by adding electrons to the already empty conduction band, can also enhance the electron stability [20,40].

- Anionic doping of TiO<sub>2</sub>

Doping TiO<sub>2</sub> with anionic nonmetals, including carbon, sulfur, nitrogen, and iodine, has been found to be more efficient in ensuring higher photocatalytic activity under visible light [26]. Anionic dopants result in p-state substitution in TiO<sub>2</sub> by altering the atomic level in the valance band and subsequent shift of the conduction band. For instance, incorporation of carbon into TiO<sub>2</sub> contributes to the formation of carbonaceous species on the surface, which increases the visible light absorption [18,58,60]. Furthermore, the presence of more reactive sites, which facilitate the adsorption of more target contaminants, is another explanation for the increase in photocatalytic activity of C-doped TiO<sub>2</sub> due to its higher surface area [26]. Nitrogen doping in TiO<sub>2</sub> adjusts the stiffness, elastic modulus, refractive index, electrical conductivity, and photocatalytic behavior of TiO<sub>2</sub> under visible light absorption activity [18].

Subsequently, silica is reported to have higher surface area, which provides the effective adsorption and catalyst support structure for heterogeneous photocatalysis. According to Ghosh and Das [26], silica modified TiO<sub>2</sub> is more effective as a photocatalyst than TiO<sub>2</sub> alone. Thus, doping TiO<sub>2</sub> with silica can enhance and stabilize both the external and internal surfaces of the catalyst within the silica-based matrix, where contaminants are adsorbed. Zeolite is also found to play an important role in charge and electron transfer during the photocatalytic reaction [20,34]. Due to uniform pores and straight paths, zeolites have been found to be good photocatalyst supports. The zeolite acts as a supporting material for the homogeneous dispersion of TiO<sub>2</sub> particles on its surface, which improves TiO<sub>2</sub>-based zeolite composites. Activated carbon (AC), due to its pore structure, also has benefits as a photocatalyst support for promoting the photocatalytic process [25,53,64]. AC is commonly used as a supporting material to extract organic and inorganic pollutants from water and wastewater. Contrariwise, the surface chemistry of AC carbon may obstruct effective coating of TiO<sub>2</sub> photocatalysts [64]. However, the application of AC–TiO<sub>2</sub> photocatalysts in wastewater treatment settings comes with a cost and, therefore, necessitates the use of a reactor to effectively expose the photocatalytic surface to light photons [2,53,64].

- Other supporting metallic oxides

Coupling TiO<sub>2</sub> with other semiconductors to increase its photocatalytic activity is another way to produce photoinduced electron–hole pairs [26]. A good match between the conduction and valence bands of two semiconductors ensures a potential charge carrier movement from one to the other. Several studies have indicated that TiO<sub>2</sub> photocatalytic activity can be enhanced by the presence of metal oxides like CdS, ZnO, ZrO<sub>2</sub>, Cu<sub>2</sub>O, CeO<sub>2</sub>, SnO<sub>2</sub>, WO<sub>3</sub>, and Fe<sub>3</sub>O<sub>4</sub> [17,18,26,62,65,66]. Among them, Fe<sub>3</sub>O<sub>4</sub> has been studied extensively due to its ability to facilitate magnetic separation of the nanocomposite from the aqueous medium [39,67]. Ahangar et al. [60] prepared a Fe<sub>3</sub>O<sub>4</sub>-embedded SiO<sub>2</sub> nanocomposite and compared its magnetic properties with pure Fe<sub>3</sub>O<sub>4</sub>. It was found that the Fe<sub>3</sub>O<sub>4</sub> nanoparticles embedded in SiO<sub>2</sub> have a much higher photocatalytic efficiency. Furthermore, the photocatalytic performance of the resulting nanocomposite was nearly identical. As a result, the core–shell framework is an efficient way to incorporate the desirable properties of two or more nanomaterials into a single nanocomposite. However, adding semiconductor dopants can alter the surface properties of TiO<sub>2</sub> catalysts, such as surface area and surface acidity [16,41]. Wang et al. [68] used a hydrothermal method followed by co-precipitation to develop anatase-structured TiO<sub>2</sub> nanoparticles (Fe/TiO<sub>2</sub>) with elongated morphological characteristics.

### 2.1.2. Mechanism of TiO<sub>2</sub> Photocatalysis

The heterogeneous photocatalysis mechanism involves the ability of semiconductors to produce charge carriers under light irradiation, preceded by the production of free radicals such as OH<sup>•</sup>, which contributes to further reactions, eventually forming CO<sub>2</sub> and H<sub>2</sub>O [32]. Excitation, bulk diffusion, light-induced surface transfer, and photon absorption with a potential energy greater than the band gap are all part of the basic photocatalytic activation mechanism [30,47]. As shown in Figure 3, when UV light with an energy greater than the band gap energy of TiO<sub>2</sub> is irradiated, electrons in the valence band are excited to the conduction band, which leaves positive charge holes (h<sup>+</sup>) in the valence band.

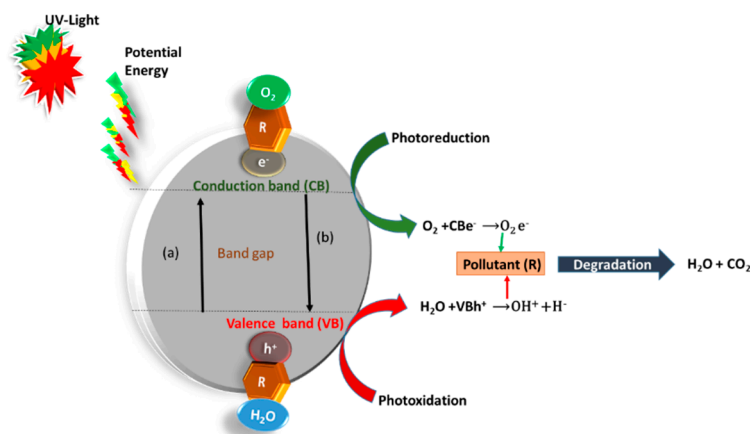
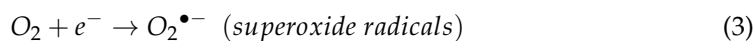
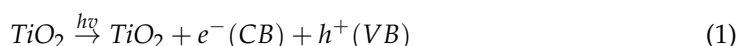


Figure 3. Schematic presentation of the photocatalysis mechanism; adapted from [26].

The electrons extracted from the VB are passed to the CB, which then react with the absorbed oxygen (O<sub>2</sub>) on the TiO<sub>2</sub> surface. As a result, a positive area (h<sup>+</sup>) forms in the VB holes and causes free electrons (e<sup>-</sup>) to form in the CB. Simultaneously, the holes (h<sup>+</sup>) react with water molecules (H<sub>2</sub>O) adsorbed on the TiO<sub>2</sub> surface to create hydroxyl radicals (OH<sup>•</sup>), as shown in Figure 3 and Equations (1)–(4). Furthermore, the CB electron reduces oxygen to superoxide ions (O<sub>2</sub><sup>•-</sup>). This reaction prevents the e<sup>-</sup>/h<sup>+</sup> from recombining, which happens when other electron acceptors such as pollutants are absent [30,40]. Organic pollutants (R) in wastewater can be oxidized to carbon dioxide (CO<sub>2</sub>) and water (H<sub>2</sub>O) by oxygen reactive radicals.



### 2.2. Operational Parameters in Photocatalysis

The photocatalytic system's oxidation rates and semiconductor catalyst performance coupled with a photoreactor are all highly dependent on several operational parameters that regulate the kinetics [18,26,69]. Outstanding studies of the different parameters affecting the photocatalysis process, including pH, catalyst loading, amount of oxygen, contaminant loading, light intensity and duration of light irradiation, preparation method of the catalyst, its calcination temperature, and amount and type of dopant, have been carried out and reported in the literature [18,25,26,51,53,70,71]. In comparison to immobilized films, photocatalysts mostly take the form of suspended powder (slurries), giving higher efficiency [25]. However, separating photocatalysts from treated water in this form is difficult, implying that a recovery step for photocatalyst re-use is required [72–74]. Pho-

photocatalysts based on  $\text{TiO}_2$  with a large surface area have a high photocatalytic efficiency, so nano-sized  $\text{TiO}_2$  particles have been used in most studies [25,74].

- pH

pH affects the surface charge or isoelectric point of the photocatalyst directly as well as the catalyst particles, size of catalyst aggregates, and the positions of conduction and valence bands [75,76]. The point of zero charge (PZC) of  $\text{TiO}_2$  is the main parameter used to study the effect of pH in photocatalyst reactions. PZC is a condition where the surface charge of  $\text{TiO}_2$  is zero or neutral in the range of 4.5–7.0 [69,75]. The catalyst surface will be negatively charged and repel the anionic compounds in water, which can affect the charge densities [75]. At pH = PZC, the neutral surface charge of the catalyst particles will not be able to produce the interactive rejection necessary for the separation of the solid liquid. When this happens, the catalyst becomes larger, thereby leading to the sedimentation of the catalyst. Since this can induce the aggregation of the catalyst, optimization becomes necessary [76].

- Catalyst loading

One of the key factors affecting photodegradation efficiency and overall cost is the amount of catalyst used. Increasing the  $\text{TiO}_2$  load does not only increase the number of active sites for pollutant adsorption, but it also increases the number of  $e^-/h^+$  pairs, which speeds up the reaction rate [18,19,75]. However, if the amount of  $\text{TiO}_2$  is increased above a saturation level, the catalyst may agglomerate, resulting in a light screening deficiency [69,75]. This makes the excess  $\text{TiO}_2$  particles reduce the active surface area of the  $\text{TiO}_2$  exposed to illumination and consequently reduces the photocatalytic efficiency. Thus, the absence or obstruction of the irradiated light prevents it from penetrating the effluent's interior mass, hence hindering photocatalysis [69]. Therefore, in order to avoid excessive usage and gain optimal photonic efficiency, an optimal value of catalyst dosage must be used [76].

- Light intensity

The light intensity ensures that sufficient photons of energy are delivered to the  $\text{TiO}_2$  surface-active sites. This should be significant enough to achieve a reasonable photocatalytic reaction rate, particularly in water treatment [51,69]. This is usually limited to photons with wavelengths that are smaller than the absorption edge of nearly 400 nm [51]. However, attenuation of radiation reaching the photocatalyst is one of the reasons for lower efficacy. Attenuation can occur for a variety of reasons, including insufficient light spatial distribution within the reactor, reflection losses, transmission losses, scattering, and so on [18,25]. According to Naldoni et al. [51], the rate of reaction can be associated with the high thermodynamic efficiency of reactor photons distributed within it.

- Catalyst type and temperature

The development of visible/solar light-active photocatalysts has been a continued effort in recent years [19,25,77,78]. Some of these photocatalysts have been synthesized and their efficacy in wastewater treatment has been determined. Additionally, most of the early photocatalysts developed were UV-only active and, therefore, research into photocatalysts' physical and chemical properties is required to support their future prospective use. Modification of  $\text{TiO}_2$  with promising results has been reported as a solution. Some researchers have worked on incorporating activated carbon, graphite, graphene oxide, nanosheets, and other elements into  $\text{TiO}_2$  while others have focused on the incorporation of various metallic and nonmetallic additives [18,19,25,51,77,79,80]. Furthermore, doping metals and nonmetals into conventional photocatalysts enhances photoreactivity, and thus quantum efficiency, by altering the intrinsic and surface properties in a favorable approach [51]. In photocatalytic activity, temperature seems to have no effect. The ideal temperature range initiated by photon adsorption reaction is reported to be 20 to 80 °C [25]. Meanwhile, the activation energy, being relatively stable at these temperatures, makes it possible for a wide

range of photon-induced reactions. However, an increase in temperature above 80 °C has been reported to have negative consequences on the overall photocatalytic process [25,51].

- Dissolved oxygen and contaminant concentration

The presence of dissolved oxygen (DO) is critical in TiO<sub>2</sub> photocatalysis. The DO ensures that there are enough electron scavengers present to aid in the trapping of the excited conduction-band electrons during the recombination step [18,51,77]. The presence of DO has no effect on the adsorption onto the TiO<sub>2</sub> catalyst surface since the reduction reaction occurs at several sites separate from where the oxidation occurs. The DO influences the formation of reactive oxygen species, the stabilization of radical intermediates, mineralization, and direct photocatalytic reactions [77]. The total amount of DO produced in a reactor is determined by a few factors such as the environmental condition, the catalyst type and concentration, the contaminant, and so on [80]. The pollutant's initial concentration has a significant impact on its photodegradation. The effectiveness of photodegradation decreases as the initial concentration increases for two reasons: (i) equilibrium adsorption of the pollutant rises with increasing concentration and thus competes with adsorption of OH<sup>−</sup> on the same site, and (ii) high-concentration pollutants absorb more than the photocatalyst itself, which tends to prevent degradation [25].

### 3. Integrated Photocatalytic Membrane (IPM) Reactors

Membrane separation has become one of the most improved technologies for water treatment in recent decades due to its small carbon footprint, high separation efficiency, and ease of operation [2,39,71]. Membrane fouling is caused by the formation of a cake layer on the membrane surface and results in pore blocking in conventional membrane processes [81]. As a result, water flux is reduced significantly, and energy consumption and treatment costs are increased. Furthermore, membrane filtration can only concentrate contaminants into a high concentration retentate, which requires additional treatment prior to discharge [39,81,82]. Therefore, advancements in membrane science and technology are useful in developing a cost-effective membrane process. In essence, membrane technology has progressed to the point where there is a plethora of membranes made for specific pollutants as well as membrane configurations and technologies tailored for specific industries (milk production, beer production, desalination, solvent separation) and material regeneration [2,4,18,25,83].

Moreover, membranes are classified according to their pore sizes as microfiltration (MF), ultrafiltration (UF), nanofiltration (NF), and reverse osmosis (RO), which determine their selectivity [25,82,83]. Nanoporous membranes (0.1–1 nm) are made up of a thin film through which molecules are transported via solution diffusion. The driving forces across such membrane transport include pressure, concentration, or potential gradient [2,25,61]. Reverse osmosis (RO), NF and most recently forward osmosis (FO) are processes that use nonporous membranes. Microfiltration (MF) and ultrafiltration (UF) are two pressure-driven processes that use microporous membranes. MF membranes can separate particles with diameters ranging from 0.1 to 10 μm, while UF membranes can remove particles with diameters ranging from 1 to 100 nm [2,84].

Generally, to meet strict wastewater discharge standards, a conventional activated sludge process is used to biologically treat wastewater for organic/nutrient removal, accompanied by an MF/UF process to produce high-quality permeate water (i.e., removing particles and bacteria/viruses, etc.) Furthermore, membrane filtration can only trap contaminants in a high concentration retentate, which requires additional post-treatment prior to discharge. In contrast, photocatalytic membrane processes may degrade contaminants in feed solutions by producing oxygen-reactive radicals in the presence of UV light, preventing the formation of a cake layer on the membrane surface [3,45]. As a result, pore blocking is reduced, pollutant concentrations in the filtrate are reduced, and permeate quality is improved [3,45]. This section delves into the different types of membranes used as supports as well as related photocatalytic membrane types, preparation, attributes and applications of TiO<sub>2</sub> photocatalytic membranes in removing contaminants in wastewater settings.

### 3.1. Types of IPM Reactors

Simple photocatalytic reactors that use  $\text{TiO}_2$ -coated glass beads and a UV lamp to illuminate and activate sites are referred to as slurry/immobilized photocatalytic reactors or fixed-bed photocatalytic reactors [16,48,82]. In recent years, photocatalytic reactors have been upgraded in a variety of ways to increase the irradiated surface area and boost performance. Consistently, the difficulty in separating nano sized  $\text{TiO}_2$  particles from treated water has been attributed to its restricted use. To solve the separation problem, some researchers have attempted to salvage nano sized  $\text{TiO}_2$  particles from suspensions using membrane filtration [20,39,48,63,82,85].

IPMs are classified into four different configurations: (Figure 4a) a membrane inserted inside a photoreactor with internal walls coated with a photocatalyst such as  $\text{TiO}_2$ ; (Figure 4b) a pure  $\text{TiO}_2$  porous photocatalytic membrane; (Figure 4c) a slurry photocatalytic reactor followed by a membrane filtration unit; (Figure 4d) an inorganic or polymeric membrane submerged in a slurry photocatalytic reactor.

Among these four configurations, the photocatalytic membrane (Figure 4b) has potential advantages over the other three configurations [26,53]. Here, both the separation membrane and the  $\text{TiO}_2$  photocatalytic degradation of the organics occurs in a single unit [26]. In addition, photocatalytic membranes generally outperform conventional membranes in terms of reducing membrane fouling and improving permeate quality [85,86]. Even though the reactor configuration covers a broad range, the reactor design should ensure that the catalyst is irradiated uniformly [25]. This is because the photocatalytic surface available for the possible solutions can decrease and cause a loss in the photocatalytic efficiency.

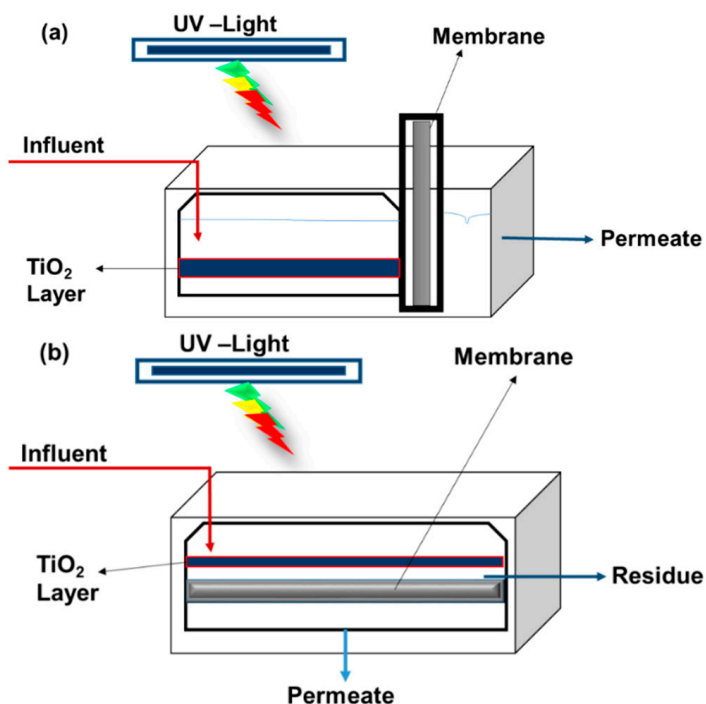
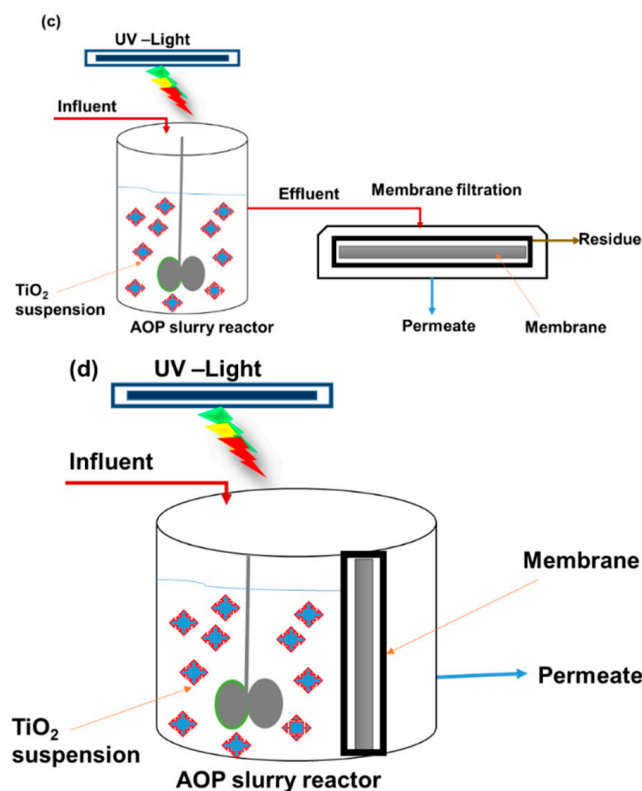


Figure 4. Cont.



**Figure 4.** Schematic diagram of TiO<sub>2</sub>-based membrane reactor types: (a) a membrane inserted inside a photoreactor with internal walls coated with a photocatalyst such as TiO<sub>2</sub>, (b) a pure TiO<sub>2</sub> porous photocatalytic membrane, (c) a slurry photocatalytic reactor followed by a membrane filtration unit, and (d) an inorganic or polymeric membrane submerged in a slurry photocatalytic reactor; adapted from [18,26,32].

Notwithstanding, IPMs have proven to be very promising in wastewater treatment settings, however, they are still limited in a large-scale application. In response, several organic, inorganic, metallic, and polymeric materials have been used as support materials in the fabrication of TiO<sub>2</sub>-based photocatalytic membrane reactors [25,26,53,70,87,88]. In contrast to immobilized TiO<sub>2</sub> membranes, TiO<sub>2</sub> nanofibers, nanowires, and nanotubes are also used to make pure TiO<sub>2</sub> photocatalytic membranes. These are classified into two major categories: (i) freestanding pure TiO<sub>2</sub> photocatalytic membrane reactors and (ii) composite TiO<sub>2</sub> photocatalytic membrane reactors [87,89,90].

### 3.2. Freestanding Pure TiO<sub>2</sub>-Based Membrane Reactors

Engineered TiO<sub>2</sub> nanoparticles have various properties that allow them to bind specific pollutants or catalyze degradation reactions when deposited or embedded on membrane surfaces [26,88,90]. However, the nanomaterial loading, matrix content, particle dispersion, nanoscale phase size, shape and orientation, as well as interactions between the phases all affect the hybrid material's overall properties [26,90]. This has inspired interest in making TiO<sub>2</sub>-engineered membranes for a variety of applications, including self-cleaning, antimicrobial thin film coatings, photocatalysis, gas sensing and dye-sensitized solar cell nanofibers with well-controlled morphology [25,26,87–90]. One-dimensional freestanding TiO<sub>2</sub> membrane reactors with various TiO<sub>2</sub> morphologies, such as nanotubes (NTs), nanofibers (NFs), and nanowires (NWs), have been developed to improve photocatalytic activity and reduce membrane fouling [31,45].

### 3.2.1. TiO<sub>2</sub> Nanotube-Based Reactors

The photocatalyst surface-to-volume ratio of synthesized TiO<sub>2</sub> NTs make them more advantageous for wastewater treatment. Some reported applications are presented in Table 3.

**Table 3.** Removal of pollutants using TiO<sub>2</sub> nanotubes.

TiO <sub>2</sub> Nanotubes	Pollutant	Removal Efficiency (%)	Reference
TiO <sub>2</sub> arrays	Acid orange 7	77	[91]
TiO <sub>2</sub> -Au/Ag	Acid orange 7	85	[91]
TiO <sub>2</sub>	Acid orange 7	99	[91]
TiO <sub>2</sub>	Oil	99	[92]
TiO <sub>2</sub> /CdS	Rhodamine B	60	[75]
Ag-TiO <sub>2</sub> /HPA/Al <sub>2</sub> O <sub>3</sub>	Humic acid	88	[47]
TiO <sub>2</sub>	Humic acid	98	[47]
Si-doped TiO <sub>2</sub>	Reactive Red ED-28	40	[83]
TiO <sub>2</sub>	Methylene blue	68	[83]
Silica/TiO <sub>2</sub>	Direct black 168	85	[83]

Although TiO<sub>2</sub> NTs are available in both crystalline and amorphous forms to enhance performance, high-temperature annealing is required to convert the amorphous form to crystalline [83,91]. For example (Figure 5), from a two-electrode electrochemical cell with titanium foil as the working electrode, a freestanding TiO<sub>2</sub> NT was synthesized using an anodization method.

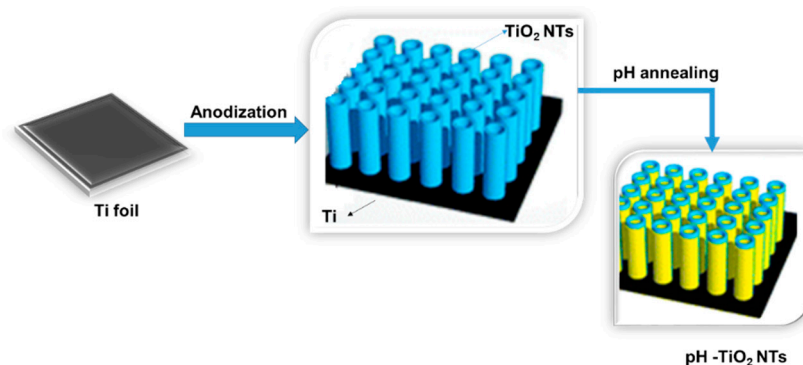


**Figure 5.** Schematic modification of TiO<sub>2</sub> nanotubes; adapted from [83,92].

In the preparation of TiO<sub>2</sub> NTs, Cai et al. [83] stated that voltage pulses were applied for a short time at the end of the anodization process to achieve open nanochannels; this was a quick and successful bottom-opening method that did not involve the use of engraving solutions. Another method for creating a TiO<sub>2</sub> nanotube alumina membrane was represented by Wang et al. [89], where the TiO<sub>2</sub> NTs were developed by immersing the alumina membrane in a 2.2 pH titanium tetrafluoride (TiF<sub>4</sub>) aqueous solution. Their reported SEM image results showed that the TiO<sub>2</sub> NTs were grafted and lined inside the channels of the alumina membrane. Chong et al. [84] reported that the effect of nanotube packing and grafting was highly dependent on the pH of the solution. Additionally, grafting time can be used to monitor TiO<sub>2</sub> NT inner diameter, with a longer grafting time resulting in a smaller internal diameter and therefore, a lower pure water flux [91,92].

### 3.2.2. TiO<sub>2</sub> Nanofiber-Based Membranes

Many methods of synthesis of TiO<sub>2</sub> nanofibers (NF) have been developed, including sol-gel, hydrothermal, and electrospinning techniques (Figure 6).

Electrospinning is a versatile and efficient technique for synthesizing uniform fibers with a broad specific surface region [28,89,93]. In electrospinning, a polymer solution or melt containing a precursor salt of metal oxide in a syringe is subjected to a high

static voltage [94,95]. The properties of nanofibers can be tweaked to provide more versatility in the end-product's surface functionalities. Many studies use Ti-alkoxides and Ti-halides as  $\text{TiO}_2$  precursors, but these are insoluble in water [65,89,94–98].  $\text{TiO}_2$  nanofibers made from water-soluble precursors make it possible to combine  $\text{TiO}_2$  with other metal oxides via water-soluble precursors [99]. At a voltage of 30 kV, nanofibers are electrodeposited, collected and dried at a temperature of 25 °C. Liu et al. [100] fabricated silver (Ag) nanoparticle-decorated  $\text{TiO}_2$  nanofiber ( $\text{TiO}_2/\text{Ag}$  NF) membranes using the polyol synthesis mechanism. The Ag-decorated membrane ( $\text{TiO}_2/\text{Ag}/\text{CdS}/\text{Ag}$  NF) was obtained by immersing  $\text{TiO}_2/\text{Ag}/\text{CdS}$  nanofibers in an algae solution for 72 h [98,100].

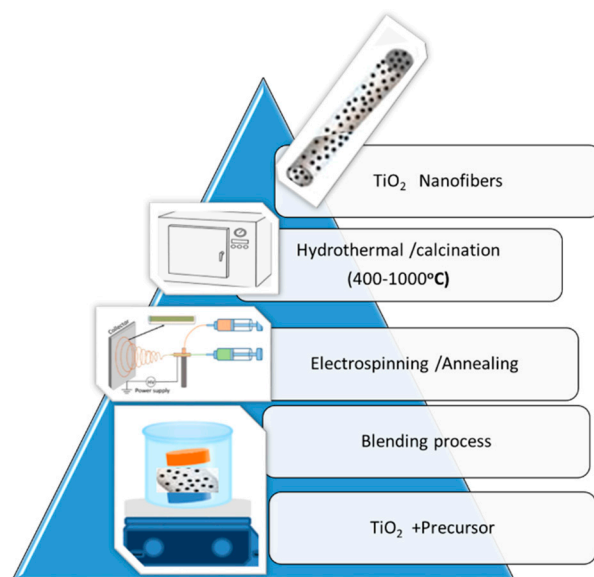


**Figure 6.** Schematic modification of  $\text{TiO}_2$  nanofibers using electrospinning and hydrothermal techniques; adapted from [98,100].

### 3.2.3. $\text{TiO}_2$ Nanowires

The successful synthesis of titanium dioxide nanowires (NWs) was achieved using a novel approach based on a hydrothermal process [101,102]. A novel  $\text{TiO}_2$  nanowire nanostructure (Figure 7) was developed by hydrothermally treating  $\text{TiO}_2$  nanopowder as a precursor for 6 h with highly concentrated sodium hydroxide [102]. In the thermal evaporation processes reported in the literature, the sputtering of a Ti buffer layer and the evaporation of Ti at high temperatures are considered mandatory [102–104]. These processes require a lot of energy and a sophisticated setup for the nanostructures to expand [101]. The thermal oxidation method has been used to produce  $\text{TiO}_2$  NWs in recent studies [102,103]. The development of  $\text{TiO}_2$  NWs with a stable rutile phase is possible with this method. Zhang et al. [102] demonstrated that a direct oxidation of a Ti foil in an organic atmosphere was possible to develop a membrane filtration process and photocatalytic degradation of humic acid in wastewater.

### 3.3. Composite $\text{TiO}_2$ Photocatalytic Membrane Reactors

$\text{TiO}_2$  composite membrane reactors are classified based on the types of support materials used on the membrane. Among these are  $\text{TiO}_2$  polymer composite membranes,  $\text{TiO}_2$  ceramic composite membranes and  $\text{TiO}_2$ -inorganic/organic materials composite membranes [82,105]. The  $\text{TiO}_2$  NPs can either be deposited onto the membrane surface or dispersed in the polymer dope solution prior to membrane casting.

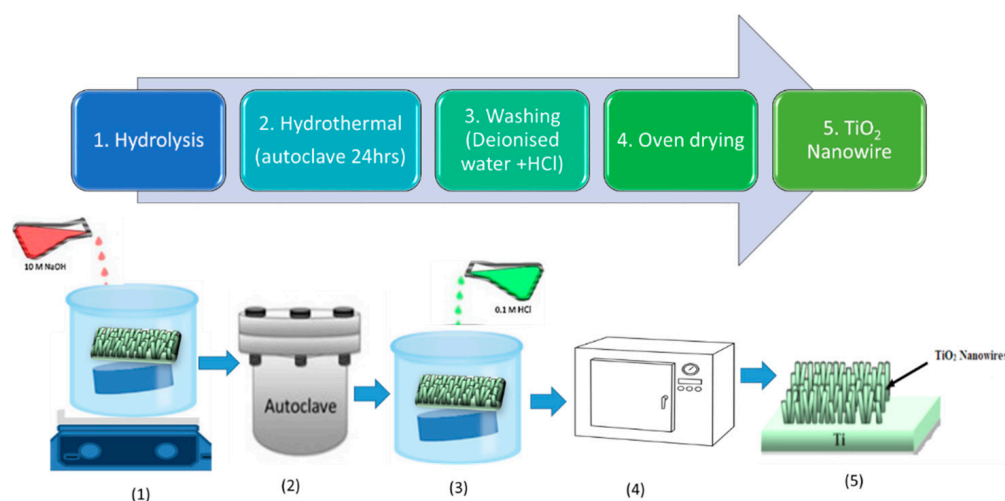


**Figure 7.** Schematic modification of TiO<sub>2</sub> nanowire using hydrothermal techniques. (1) Hydrolysis, (2) Hydrothermal, (3) Washing, (4) Oven drying and (5) TiO<sub>2</sub> nanowire.

### 3.3.1. TiO<sub>2</sub> Nanoparticle-Coated Polymer Membranes

In photocatalytic membranes, nanoscale inorganic/organic photocatalysts are embedded in a membrane matrix to improve the properties of the resulting polymer [82,105–107]. Hamed et al. [108] elucidated that TiO<sub>2</sub> nanoparticles can coordinate with the surface of the polymer membrane and Ti<sup>4+</sup> makes ion connections with oxygen atoms of carboxylic groups of polymers or by making H-bonding with carbonyl or hydroxyl groups on the TiO<sub>2</sub> surface. Hyeok et al. [109] increased the hydrophilicity of a commercial membrane via plasma immersion in a nitrogen-purged aqueous acrylic acid solution at various concentrations. The plasma treatment irradiated the membrane surface, causing radicals to form and promoting grafting reactions. TiO<sub>2</sub> was then successfully deposited onto the functionalized membrane surface [82,105].

Some researchers have investigated the photocatalytic behavior of TiO<sub>2</sub> nanoparticles photografted onto commercial polymer membranes, such as polyester membranes [24,82,108,110]. Dong et al. [98] used the activation reaction to coat TiO<sub>2</sub> nanotubes on a polyurethane (PU) membrane surface. The TiO<sub>2</sub> nanotube suspension was formed by ultrasonically dissolving salinized TiO<sub>2</sub> nanotubes in toluene for 10 min. The activated PU membrane was added to the coating process, which was then heated to 60 °C. Furthermore, the TiO<sub>2</sub> nanotube–PU hybrid membrane was collected and washed in ethanol before being dried in a vacuum oven. When the membranes were modified with diethanolamine (DEA), Hamed et al. [108] found that a high concentration of TiO<sub>2</sub> coated on the polyvinylidene fluoride (PVDF) membrane improved pure water flux. Although embedding nanoparticles onto membranes remove unwanted nanoparticles after treatment, the polymer phase material covering the nanoparticles can reduce the active usable surface area [107]. Owing to the blockage of the membrane pores by TiO<sub>2</sub> nanoparticles, the photocatalytic membrane's pure water flux usually decreases as the concentration of TiO<sub>2</sub> in the coating phase rises [58,107,109,111].

### 3.3.2. TiO<sub>2</sub>-Based Polymeric Membranes

Polymer membranes are one of the most popular membranes used in wastewater treatment and water purification (Table 4).

**Table 4.** Polymer membranes with different TiO<sub>2</sub> types.

Polymer Membrane	Types of TiO <sub>2</sub>	Deposition Time (min)	Reference
Polyethersulfone (PES) Ultrafiltration membrane	Degussa 25	15–30 60	[112]
Poly (vinylidene fluoride) Plasma-grafted poly acrylic acid (PAA)	TiO <sub>2</sub> suspension	30	[113]
Polyamide thin film supported on polysulfide	TiO <sub>2</sub> colloidal solution	60	[107]
Polyether sulfone (PES) Polyimide blend membrane (PI)	Degussa 25	15	[109]

Polymers reported as support membranes of photocatalysts include polyamide, polyvinylidene fluoride (PVDF) [23], polyethersulfone (PES), poly (vinylidene fluoride) (PVDF) [24], sulfonated polyethersulfone (SPES), poly (vinylidene fluoride) [105–108], polyurethane (PU) [98], polyethylene terephthalate (PET) [82], polyester [58], polyacrylonitrile (PAN) [43] and polytetrafluoroethylene (PTFE) [109–114]. Polymer–inorganic nanoparticle composite membranes can be divided into two groups based on their structure: (a) polymer and inorganic phases linked by covalent bonds, and (b) polymer and inorganic phases linked by van der Waals forces or hydrogen bonds [113]. The TiO<sub>2</sub> nanoparticles coalesce with the surface of the polymer membrane during the membrane preparation process. Likewise, Ti<sup>4+</sup> makes ion connections with oxygen atoms of carboxylic groups of polymers or by making H-bonds with carbonyl or hydroxyl groups on TiO<sub>2</sub> surfaces [107,111].

### 3.3.3. TiO<sub>2</sub> Ceramic Membranes

Ceramic membranes, especially Al<sub>2</sub>O<sub>3</sub> membranes, have been extensively investigated as supports for photocatalyst immobilization in membrane photocatalytic processes (Table 5).

**Table 5.** Synthesized TiO<sub>2</sub> ceramic membranes.

Type of Membrane	Type of TiO <sub>2</sub> Precursor	Calcination Conditions	Reference
Al <sub>2</sub> O <sub>3</sub>	Tetra-n-butyl titanate	400 °C for 6 h by 100 °C/h	[18]
Al <sub>2</sub> O <sub>3</sub>	Tetraethyl orthosilicate	400 °C for 2 h by 100 °C/h	
ZrO <sub>2</sub>	Tetra-butyl orthotitanate	530 °C for 1 h by 100 °C/h	[20]
Al <sub>2</sub> O <sub>3</sub>	Tetra-n-butyl titanate	500 °C for 2 h by 2 °C/min	[115]
Al <sub>2</sub> O <sub>3</sub> .ZrO <sub>2</sub>	Tetraisopropoxide titanium	510 °C for 2 h by 5 °C/min	
Al <sub>2</sub> O <sub>3</sub>	Titanium tetraisopropoxide	500 °C for 15 min by 3 °C/min	[20]
Activated carbon filter	Tetra-n-butyl titanate	200 °C for 15h	[18]
Al <sub>2</sub> O <sub>3</sub>	Tetraisopropyl orthotitanate	450 °C by 10 °C/h	[20]
Al <sub>2</sub> O <sub>3</sub>	Commercial TiO <sub>2</sub>	450 °C by 0.5/min	[115]

These are more chemically, thermally and mechanically stable than polymeric membranes. A summary of comparing the ceramic and polymeric membranes is presented in Table 6.

Polymeric membranes are commonly used for the treatment of industrial wastewater due to their availability [115]. On the other hand, ceramic membranes have an advantage over other wastewater treatment options because of their chemical and thermal stability [18,20,115]. Ceramic membranes, for example, can withstand high chlorine doses and work between pH levels of 1 to 14 and temperatures of up to 500 °C. Despite the advantages of ceramic membranes over polymeric membranes, their use has been restricted due to their high initial cost [20].

**Table 6.** Comparison of different types of membranes; adapted from [116].

Membrane Type	Polymeric Membrane		Ceramic Membrane
Membrane morphology	Hollow fiber	Flat sheet	Tubular membrane
Stability	Medium	Medium	Good
Price	Less expensive	Less expensive	Expensive
Configuration mode	Internal or external	Internal or external	Internal or external
Module processing	Quite simple	Easy	Hard

### 3.4. TiO<sub>2</sub>-Based Membrane Modification Techniques

TiO<sub>2</sub>-based catalysts can be deposited on structured membranes through aqueous or gaseous routes [117]. Membranes with desired morphology and properties are prepared using sol–gel, immersion precipitation, vapor-mediated phase separation and immersion precipitation, electrospinning, dip-coating, sintering, track-etching, stretching, template-leaching, and phase-inversion techniques [71,86,87,90,108,112,113]. Aqueous or gaseous routes can also be used to deposit TiO<sub>2</sub>-based catalysts on standardized membranes. The advantages and drawbacks of various methods for immobilizing TiO<sub>2</sub> catalysts on membranes are summarized in Table 7.

**Table 7.** Advantages and disadvantages of different methods used for immobilizing TiO<sub>2</sub> photocatalysts [116,117].

Synthesis Technique Type	Advantage	Disadvantage
Chemical vapor deposition	Processing time is short. Suitable for high-deposition-rate uniform films.	High deposition temperature (>600 °C) is required. Due to varying evaporation times, deposition of many sources of precursors is difficult. When a vacuum system is used, the price skyrockets.
Physical vapor deposition	Low-to-medium deposition temperature (<600 °C) required. Does not involve complex chemical reactions.	Expensive as vacuum systems are used. Deposition of multiple sources of precursors are difficult.
Sol–gel	High purity of materials Homogeneity is achievable. Versatile means processing and control of parameters. Large surface area materials are produced. Chemical bonding results in strong adherence of coating to the substrate.	Hydrolysis rate is difficult to control.  Longer processing time required.  Calcination at higher temperatures is required.

Among them, the sol–gel method is the most used method for making TiO<sub>2</sub> photocatalysts and subsequent incorporation of membrane matrices. This method is notable for producing unique stable structures at low temperatures as well as for its excellent chemical homogeneity [85,108,113]. Controlling the precursor chemistry and processing conditions will tailor the compositional and microstructural properties of nano-sized samples. As precursors, inorganic metal salts such as titanyl sulphate, titanium tetrachloride and others (non-alkoxide), and metal alkoxides such as titanium (IV) butoxide are commonly used [90,118]. The pH of the reaction medium, the water/alkoxide ratio, and reaction temperatures can influence the sol–gel phase. Horovitz et al. [119] prepared a TiO<sub>2</sub> sol by stirring an ethanol solution in an ice bath while adding a specific amount of TiO<sub>2</sub> precursor.

The second solution was gradually added with a 50:1:3 volume ratio of ethanol, water, and acetic acid. The mixed solution was held at 20 °C for 30 min before being ultrasonicated to produce a visible TiO<sub>2</sub> sol. Dip-coating was achieved by immersing a substrate membrane in the sol for a set period and then drying the coated membrane [71,86]. Penboon et al. [85] made a distinction between TiO<sub>2</sub>-coated membranes and TiO<sub>2</sub>-blended polymer membranes. It was deduced that the TiO<sub>2</sub>-blended membranes had a more porous structure, but the coated TiO<sub>2</sub> composite membranes had greater antifouling properties and long-term flux stability. They went on to say that TiO<sub>2</sub> nanoparticles, which were spread on the membrane's surface using the coating process, could minimize pore blockage. Furthermore, TiO<sub>2</sub>-coated membranes are more hydrophilic than TiO<sub>2</sub>-blended membranes.

### 3.5. Characteristics of Photocatalytic Membranes

Characterization of photocatalytic membranes is based on two parameters, membrane morphology and efficiency (permeability, flux, rejection, and separation factors), which are used to describe the membranes (pore size, pore size distribution, thickness of membrane, charge density and pore shape, chemical properties, and physical properties) [3,18,120]. Improving the hydrophilicity of the membrane surface for TiO<sub>2</sub> nanoparticle deposition involves the introduction of functional groups to the membrane matrix (Table 8).

On the other hand, little research has been done on the impact of immersion time on the properties of photocatalytic membranes. According to Zhang et al. [121], longer immersion periods resulted in more TiO<sub>2</sub> nanoparticles coating the membrane surface, which appeared to clog the membrane pores and reduce flux. Nanomaterials and membranes must be characterized in order to understand their structure, chemistry, morphology, surface charge, wet potential, tensile strength and selectivity for a particular application [39,71,82,112]. Notwithstanding, membrane efficiency degrades over time due to a variety of factors such as fouling, chemical contamination, disintegration and cleaning. Therefore, characterization in this case using particular techniques provides useful information about membrane structure and topography in order to gain insight into performance loss or affected membrane structure.

Similarly, modified membranes (modification with nanomaterials) are also characterized in order to better understand the modified surface layer and how it affects membrane performance. Commonly used techniques and methods for characterization include scanning electron microscopy (SEM), transmission electron microscopy (TEM), Fourier transform infrared spectroscopy (FTIR), X-ray diffraction (XRD), X-ray photo electron spectroscopy (XPS), thermogravimetric analysis (TGA), energy dispersive X-ray spectroscopy (EDX), dynamic light scattering (DLS), contact angle, porosity, and zeta potential (Table 8). Thiruvengkatchari et al. [19] reported that after 30 min of reverse osmosis-pressurized activity, some TiO<sub>2</sub> particles detached from the membranes, but no further loss occurred after 7 days that was evidently noticeable in SEM images. Koseoglu-Imer and Koyuncu [105] eluded that diethanolamine increased the hydroxyl groups on the membrane surface, lowering the steric hindrance for attracting TiO<sub>2</sub> nanoparticles. The content of TiO<sub>2</sub> on the DEA-modified membrane was three times higher than on the membrane without DEA, according to the results of energy disperse X-ray spectroscopy.

Furthermore, membrane fouling is the accumulation of macromolecules (polysaccharides, proteins), colloids, microorganisms (bacteria, viruses) and salts (multivalent/monovalent) on the surface or within the pores of a membrane [45,113]. Fouling has a few significant drawbacks in membrane technology, including a reduction in permeation flux, a change in selectivity, and a reduction in membrane life during filtration. Membrane fouling is categorized into inorganic fouling, colloidal fouling, organic fouling and biofouling [45,113,118,122]. Therefore, developing photocatalytic membranes (fouling resistant membranes) are a safer alternative for fouling mitigation since they reduce foulant coagulation on the membrane surface, which contributes to clogging.

**Table 8.** Modification and characterization techniques of TiO<sub>2</sub>-based membranes.

Membrane Types	Modification Methods	Characterization Methods	Reference
TiO <sub>2</sub> -Polysulfone (PS)	Blending	FTIR, SEM/EDS. XRD, contact angle, zeta potential	[105]
TiO <sub>2</sub> -Polyethersulfone (PES)	Sol-gel	FTIR, XRD, SEM/EDS	[118]
TiO <sub>2</sub> /PES	Phase inversion	Contact angle, FT-IR, TGA, pore size distribution, SEM	[123]
TiO <sub>2</sub> /Cellulose Acetate	Dip-coating	Contact angle, viscosity, SEM, FTIR	[113]
ZrO <sub>2</sub> PVDF	Blending	SEM, TEM, AFM, XPS, TGA, contact angle	[95]
Cellulose acetate-Polyurethane (CA-PU)	Blending	SEM, TEM, AFM, XPS, TGA, contact angle	[19]
Polyvinylchloride (PVC)	Sol-gel	SEM, FTIR, DLS, TGA	[105]

### 3.6. Application of TiO<sub>2</sub>-Based Membranes

Photocatalytic membranes, which combine membrane filtration with photocatalytic degradation of organics and subsequent antibacterial treatment in a single system, have shown great prospects in water and wastewater treatment settings [12,123–127]. Furthermore, membrane flux is a critical parameter for the photocatalytic membrane system, as it can be enhanced by multilayered deposition of TiO<sub>2</sub> nanoparticles on the membrane surface, but pore blockage can minimize water flux in some cases [20,87]. In order to achieve the best overall performance of the membrane, the optimal balance between photocatalytic activity and membrane flux must be considered.

#### 3.6.1. Wastewater Treatment

Photocatalytic membranes are becoming more prominent to deal with emerging contaminants (antibiotics, pharmaceuticals, nanoplastics, and so on) re-routed to wastewater treatment plants, as well as pre- and post-treatment concerns [128–130]. Increased attempts to eliminate toxic contaminants and pathogens from water have come about from the need for high-quality drinking water [12,15]. Photocatalytic membranes have proven to be more effective in removing recalcitrant organic matter than conventional wastewater treatment processes such as coagulation and filtration [131]. Therefore, they have been the subject of comprehensive research over the last few decades for the removal of toxic organic and inorganic compounds from water (Table 9).

**Table 9.** Application of TiO<sub>2</sub>-based membranes in wastewater settings.

Hybrid Membranes.	Pollutants	Removal Efficiency (%)	Reference
UV-ZrO <sub>2</sub> /TiO <sub>2</sub> -Al <sub>2</sub> O <sub>3</sub>	Methylene blue	95	[25]
Solar-Ag/TiO <sub>2</sub>	Methylene blue	80	[18]
UV-TiO <sub>2</sub> /Al <sub>2</sub> O <sub>3</sub>	Direct black 168	63	[97]
UV-ZrO <sub>2</sub> /TiO <sub>2</sub> -Al <sub>2</sub> O <sub>3</sub>	Methyl orange	95	[132]
UV-TiO <sub>2</sub> /PVDF	Reactive black 5	99	[51]
UV-TiO <sub>2</sub> -Al <sub>2</sub> O <sub>3</sub>	Reactive black 5	70	[97]
UV-TiO <sub>2</sub> nanotube	Rhodamine B	70	[131]
TiO <sub>2</sub> nanotube	Humic acid	28	[112]
UV-TiO <sub>2</sub> nanowire	Humic acid	60	[102]
UV-TiO <sub>2</sub> /Al <sub>2</sub> O <sub>3</sub>	Humic acid	97	[112]
UV-TiO <sub>2</sub> nanotube	Humic acid	95	[102]

Zheng [20] reported on photocatalytic membranes for the removal of heavy metals such as mercury, lead, mercury, and cadmium from wastewater settings. Other researchers have reported that multilayered nanocomposite membranes have promising properties

for heavy metal ion adsorption, photocatalysis, self-cleaning, enhanced dye rejection performance and reduced fouling [39,61,81,82]. Batch reactors and photocatalytic polycrystalline TiO<sub>2</sub> membrane reactors were used by Shetty et al. [131] to degrade various pharmaceuticals from water at various pH levels. Due to the catalysts' different hydrophilicity/hydrophobicity at different pH levels, the substrates showed different adsorption on catalyst surfaces when the system was in recirculation mode. The treated water had a permeate flux of 31.5–60.0 L/h.m<sup>2</sup> in both the alkaline and acidic mediums, with a rejection percentage of 10–60% for furosemide and 5–30% for ranitidine [131]. Table 9 summarizes the removal of pollutants using different types of photocatalytic membranes.

### 3.6.2. Other Industrial Applications

The development and production of simple and responsive biosensors have sparked a lot of interest due to their wide range of applications, including disease detection, drug discovery, food protection and environmental monitoring [82,85,106,133,134]. Due to the small active surface area of microelectrodes and the low recognition signal, electrochemical biosensors have a difficult time working [125]. As a result, chemical and thermal stability with good biocompatibility makes TiO<sub>2</sub> appear to be a promising biosensor material [48]. Therefore, combining it with membranes would improve its suitability for environmentally friendly designs and applications. Examples of these materials include TiO<sub>2</sub> nanotubes, nanosheets, solgel matrices, and three-dimensional microporous matrices [48,71,98,125]. Chen and Zhao [39] reported their first study on the production of a Fe<sub>3</sub>O<sub>4</sub>@TiO<sub>2</sub> magnetic NP-based disposable test strip immunosensor that uses a multienzyme labeled amplification strategy to detect organophosphorus (OP) pesticides in human plasma.

## 4. Challenges and Future Prospects of Photocatalytic Membranes

Membrane-based technologies are gaining worldwide popularity in wastewater treatment settings due to their high separation efficiencies, low cost, small carbon footprint and ease of operation. This process can also be used to eliminate a wide variety of harmful pollutants, including pesticides and herbicides used in agriculture, as well as dyes and toxic metal ions used in industry. Despite extensive research and thorough studies of photocatalytic semiconductors (TiO<sub>2</sub>), many aspects of this process remain unsolved. One of the pressing issues as to whether the photocatalytic process should be used as a pretreatment or as a standalone form of water purification is the operating conditions that pose major constraints. Consequentially, the chemical composition and pH of industrial wastewater vary by region. Therefore, efforts should be made to develop photocatalytic membrane materials that can be used under a wide range or optimized operating conditions such as temperature, pH and contaminant concentrations. Furthermore, to achieve continuous irradiation with visible light over a wider range of operating conditions, a significant amount of research should be devoted to the doping and modification of TiO<sub>2</sub> and other semiconductors. However, catalyst immobilization is an obstacle that must be overcome in order to maximize the photocatalysts' irradiated surface area. This is needed to avoid issues such as catalyst recovery and agglomeration, which are very common in slurry-based photoreactors.

### 4.1. Photocatalytic Membranes

Membrane fouling, which is caused by the accumulation of anthropogenic organic contaminants and microorganisms on the membrane pores' surface, results in poor water quality, high operating costs, and a limited membrane life. In order to perform equal photocatalytic operation with minimal water flow consequences, an adequate level of photocatalysts should be incorporated into the membrane. In addition to TiO<sub>2</sub> loading, light intensity and irradiation time influence membrane quality.

In order to execute reasonable photocatalytic activity with minimal water flow repercussions, an appropriate level of the photocatalyst should be incorporated into the membrane. Membrane performance is also influenced by light intensity and irradiation time in

addition to TiO<sub>2</sub> loading. Addressing this, photocatalytic membranes have been reported to have better fouling resistance as well as antimicrobial properties. Two-dimensional nanosheets with graphene have been reported to be useful for membrane applications. Additionally, combinations of nanowires with graphene sheets have also gained attention recently. Such types of structures provide antifouling and antimicrobial properties as well as hydrophilicity and aqueous stability.

#### 4.2. Magnetized TiO<sub>2</sub> Photocatalytic Membranes

In order to implement heterogeneous photocatalysis into practical water and wastewater treatment applications, the overall cost of the process should be minimized. One of the ways to decrease the cost is to improve the recyclability of the photocatalyst. This can be achieved by introducing magnetic constituents into the photocatalytic nanocomposite to enhance recoverability by the application of an external magnetic field. Magnetic components (Fe<sub>3</sub>O<sub>4</sub>) can benefit in the recovery of photocatalyst particles by preventing them from clumping together [39,67]. Magnetite (Fe<sub>3</sub>O<sub>4</sub>) NPs, maghemite (Fe<sub>2</sub>O<sub>3</sub>) NPs and nanorods, and hexagonal ferrites are examples of ferritic nanomaterials that are simple to recover by magnetic fields and are re-usable due to their long-term stability.

In some studies, Fe<sub>3</sub>O<sub>4</sub> and TiO<sub>2</sub> nanoparticles have also been successfully used as a filler for composite membranes. This opens a broad spectrum of recycling possibilities in the form of magnetized photocatalytic membrane applications (Table 10).

**Table 10.** Examples of magnetite heterojunction photocatalyst performance.

Composition	Pollutant	Operating Condition	Efficiency (%)	Reference
Fe <sub>3</sub> O <sub>4</sub> (0.075 gL <sup>-1</sup> )	<i>E. coli</i>	UV @ <i>t</i> = 60 min	50.5	[41]
Fe <sub>3</sub> O <sub>4</sub> -TiO <sub>2</sub>	Bisphenol (10 ppm)	UV @ <i>t</i> = 60 min	92	[106]
Fe <sub>3</sub> O <sub>4</sub> -ZnO	Rhodamine B (7 ppm)	UV @ <i>t</i> = 60 min	99.3	[52]
Fe <sub>3</sub> O <sub>4</sub> -ZnO-rGO	Methylene violet (408 ppm)	UV vis @ <i>t</i> = 120 min	83.5	[52]
Bi <sub>2</sub> O <sub>3</sub> -Fe <sub>3</sub> O <sub>4</sub>	Ibuprofen (2.1 ppm)	UV vis @ <i>t</i> = 120 min	>95	[39]
Fe <sub>3</sub> O <sub>4</sub> -CuO-ZnO-nano graphene	Methylene blue (30 ppm)	UV @ <i>t</i> = 120 min	93	[67]
Fe <sub>3</sub> O <sub>4</sub> -ZnO-CoWO <sub>4</sub>	Rhodamine B (4.8 ppm)	UV vis @ <i>t</i> = 405 min	98.3	[134]
Fe <sub>3</sub> O <sub>4</sub> -Bi <sub>2</sub> O <sub>3</sub>	Ciprofloxacin	UV vis @ <i>t</i> = 240 min	98.3	[131]

Thus, Fe<sub>3</sub>O<sub>4</sub> NPs display exceptional superparamagnetic behavior, which provides an additional benefit of a much easier magnetic separation of the semiconductor and the solution. The coprecipitation method or thermal decomposition method is widely used to make Fe<sub>3</sub>O<sub>4</sub> nanoparticles, with minor variations such as room temperature (25–80 °C). The exemplary adsorption potential for toxic metal ion removal was achieved by the finite-size effect of magnetic nanoparticles with high surface-to-volume ratios [118]. Magnetite has also been used as an additive due to its unique features, such as physicochemical properties and high biocompatibility. Many polymeric-based membranes, such as polysulfide and polyether sulfone, had their membranes magnetized with magnetite to strengthen antifouling properties. However, knowledge of magnetized TiO<sub>2</sub> photocatalytic membranes is still limited and therefore requires more attention.

#### 4.3. Life Cycle Assessment (LCA)

A life cycle assessment (LCA) is needed to incorporate TiO<sub>2</sub> photocatalytic-based membrane technology on a large scale [3,84]. LCA is one of the most useful instruments for

determining a process's environmental effects as well as its viability and costs. Although there is a large amount of information in the literature about the recyclability and reusability of TiO<sub>2</sub> photocatalysts, there is still limited knowledge about their end of life [3,19]. The photocatalytic process performance, on the other hand, is highly dependent on the feed water's consistency, the operating conditions and type of treatment configuration. Apart from the environmental impacts of high organic wastewater, the amount of energy required has a major impact on the photocatalysis process [3,84]. This is one of the reasons why solar photocatalysis has received so much attention in recent years. Consequently, the toxicological and environmental impacts of a wastewater treatment facility can be detected and minimized using LCA.

## 5. Conclusions

This review study presents the photocatalytic membrane process as a game-changing technology to mitigate fouling and other drawbacks of membrane processes in addressing water scarcity and major environmental challenges. Characteristics of TiO<sub>2</sub>-based photocatalytic membranes with insight into their types, fabrication techniques, operational conditions and applications in water settings are discussed. As a result, the advancement of photocatalytic membrane reactors based on a wide range of nanomaterials and TiO<sub>2</sub> photocatalyst phase modification is anticipated to have an unparalleled future in water and wastewater treatment settings. The development of magnetite TiO<sub>2</sub> photocatalytic membranes was found to be an ecofriendly choice to increase photocatalytic and recoverability activities as well as reduce membrane fouling. Additionally, incorporating magnetized TiO<sub>2</sub> photocatalytic membranes as a post-treatment to an existing biological system can reduce eutrophication potential while increasing biomethane potential for energy usage. The prospects of life cycle assessment, research and development of magnetic photoactive-based membranes is foreseen to be economically viable with the possible potential to resolve the current membrane setbacks and bring the application of this technology to industrial scale.

**Author Contributions:** Conceptualization, E.K.T.; funding acquisition, S.R. and M.N.C.; writing draft, E.K.T.; reviewing and editing, D.A.-S., S.R., and M.N.C.; supervision: S.R.; project administration: E.K.T. and D.A.-S. All authors have read and agreed to the published version of the manuscript.

**Funding:** This research was funded by the Water Research Commission of South Africa under project identification WRC Project: C2019/2020-00212 and the National Research Foundation scholarship grant number 130143.

**Institutional Review Board Statement:** Not applicable.

**Informed Consent Statement:** Not applicable.

**Data Availability Statement:** Not applicable.

**Acknowledgments:** The authors wish to thank the Durban University of Technology, the Green Engineering and Sustainability Research Group, and the Water Research Commission of South Africa for their support on the project identification WRC Project: C2019/2020-00212. The authors also wish to thank the National Research Foundation for their scholarship grant number 130143.

**Conflicts of Interest:** The authors declare no conflict of interest. The funders had no role in the design of the study; in the collection, analyses, or interpretation of data; in the writing of the manuscript, or in the decision to publish the results.

## References

1. Tetteh, E.K.; Amankwa, M.O.; Armah, E.K.; Rathilal, S. Fate of covid-19 occurrences in wastewater systems: Emerging detection and treatment technologies—A review. *Water* **2020**, *12*, 2680. [[CrossRef](#)]
2. Zhang, J.; Tong, H.; Pei, W.; Liu, W.; Shi, F.; Li, Y.; Huo, Y. Integrated photocatalysis-adsorption-membrane separation in rotating reactor for synergistic removal of RhB. *Chemosphere* **2021**, *270*. [[CrossRef](#)]
3. Hube, S.; Eskafi, M.; Hrafnkelsdóttir, K.F.; Bjarnadóttir, B.; Bjarnadóttir, M.Á.; Axelsdóttir, S.; Wu, B. Direct membrane filtration for wastewater treatment and resource recovery: A review. *Sci. Total Environ.* **2020**, *710*. [[CrossRef](#)]

4. Schutte, C.F.; Focke, W. *Evaluation of Nanotechnology for Application in Water and Wastewater Treatment and Related Aspects in South Africa*; Water Research Commission: Pretoria, South Africa, 2007; p. 28.
5. Chollom, M.N.; Rathilal, S.; Swalaha, F.M.; Bakare, B.F.; Tetteh, E.K. Removal of antibiotics during the anaerobic digestion of slaughterhouse wastewater. *Int. J. Sustain. Dev. Plan.* **2020**, *15*. [[CrossRef](#)]
6. Anvari, A.; Amoli-Diva, M.; Sadighi-Bonabi, R. Concurrent photocatalytic degradation and filtration with bi-plasmonic TiO<sub>2</sub> for wastewater treatment. *Micro Nano Lett.* **2021**, *16*. [[CrossRef](#)]
7. Ezugbe, E.O.; Tetteh, E.K.; Rathilal, S.; Asante-Sackey, D.; Amo-Duodu, G. Desalination of municipal wastewater using forward osmosis. *Membranes* **2021**, *11*, 119. [[CrossRef](#)] [[PubMed](#)]
8. Chollom, M.N.; Rathilal, S.; Swalaha, F.M.; Bakare, B.F.; Tetteh, E.K. Anaerobic treatment of slaughterhouse wastewater: Evaluating operating conditions. *WIT Trans. Ecol. Environ.* **2019**, 239. [[CrossRef](#)]
9. della Rocca, D.G.; Peralta, R.M.; Peralta, R.A.; Moreira, R.d.P.M. Recent development on Ag<sub>2</sub>MoO<sub>4</sub>-based advanced oxidation processes: A review. *React. Kinet. Mech. Catal.* **2021**, 132. [[CrossRef](#)]
10. Ahmed, S.N.; Haider, W. Heterogeneous photocatalysis and its potential applications in water and wastewater treatment: A review. *Nanotechnology* **2018**, *29*. [[CrossRef](#)] [[PubMed](#)]
11. Qiu, X.; Zhang, Y.; Zhu, Y.; Long, C.; Su, L.; Liu, S.; Tang, Z. Applications of Nanomaterials in Asymmetric Photocatalysis: Recent Progress, Challenges, and Opportunities. *Adv. Mater.* **2021**, *33*. [[CrossRef](#)]
12. Naddeo, V.; Balakrishnan, M.; Choo, K.-H. *Frontiers in Water-Energy-Nexus—Nature-Based Solutions, Advanced Technologies and Best Practices for Environmental Sustainability: Proceedings of the 2nd WaterEnergyNEXUS Conference*; Springer Nature: Salerno, Italy, 2019.
13. Wang, Z.; Wang, L.; Yao, L.; Pei, M.; Zhang, G. Membrane separation coupled with photocatalysis for water supply and wastewater treatment. *Adv. Mater. Res.* **2013**, 671–674, 2571–2574. [[CrossRef](#)]
14. Molinari, R.; Argurio, P.; Szymański, K.; Darowna, D.; Mozia, S. Photocatalytic membrane reactors for wastewater treatment. In *Current Trends and Future Developments on (Bio-) Membranes: Membrane Technology for Water and Wastewater Treatment Advances and Emerging Processes*; Elsevier: Amsterdam, The Netherlands, 2020.
15. Cai, Z.; Dwivedi, A.D.; Lee, W.N.; Zhao, X.; Liu, W.; Sillanpää, M.; Zhao, D.; Huang, C.H.; Fu, J. Application of nanotechnologies for removing pharmaceutically active compounds from water: Development and future trends. *Environ. Sci. Nano* **2018**, *5*. [[CrossRef](#)]
16. Li, Q.; Kong, H.; Jia, R.; Shao, J.; He, Y. Enhanced catalytic degradation of amoxicillin with TiO<sub>2</sub>-Fe<sub>3</sub>O<sub>4</sub> composites: Via a submerged magnetic separation membrane photocatalytic reactor (SMSMPR). *RSC Adv.* **2019**, *9*. [[CrossRef](#)]
17. Lavorato, C.; Argurio, P.; Molinari, R. TiO<sub>2</sub> and Pd/TiO<sub>2</sub> as Photocatalysts for Hydrogenation of Ketones and Perspective of Membrane Application. *Int. J. Adv. Res. Chem. Sci.* **2019**, *6*, 33–41. [[CrossRef](#)]
18. Indonesia, G.B. Development of TiO<sub>2</sub> Nanoparticles/Nanosolution for Photocatalytic Activity. Ph.D. Thesis, Universiti Sains Malaysia, Penang, Malaysia, 2015.
19. Thiruvengkatachari, R.; Vigneswaran, S.; Moon, I.S. A review on UV/TiO<sub>2</sub> photocatalytic oxidation process. *Korean J. Chem. Eng.* **2008**, *25*, 64–72. [[CrossRef](#)]
20. Zheng, Z. Synthesis and Modifications of Metal Oxide Nanostructures and Their Applications. Ph.D. Thesis, Queensland University of Technology Brisbane Australia, Brisbane, Australia, 2009; p. 27.
21. Nemiwal, M.; Zhang, T.C.; Kumar, D. Recent progress in g-C<sub>3</sub>N<sub>4</sub>, TiO<sub>2</sub> and ZnO based photocatalysts for dye degradation: Strategies to improve photocatalytic activity. *Sci. Total Environ.* **2021**, 767. [[CrossRef](#)] [[PubMed](#)]
22. Cheng, M.; Zeng, G.; Huang, D.; Lai, C.; Xu, P.; Zhang, C.; Liu, Y. Hydroxyl radicals based advanced oxidation processes (AOPs) for remediation of soils contaminated with organic compounds: A review. *Chem. Eng. J.* **2015**, *4*, 582–598. [[CrossRef](#)]
23. Luo, H.; Yan, M.; Wu, Y.; Lin, X.; Yan, Y. Facile synthesis of PVDF photocatalytic membrane based on NCQDs/BiOBr/TiO<sub>2</sub> heterojunction for effective removal of tetracycline. *Mater. Sci. Eng. B Solid-State Mater. Adv. Technol.* **2021**, 265. [[CrossRef](#)]
24. Choi, H.; Sofranko, A.C.; Dionysiou, D.D. Nanocrystalline TiO<sub>2</sub> photocatalytic membranes with a hierarchical mesoporous multilayer structure: Synthesis, characterization, and multifunction. *Adv. Funct. Mater.* **2006**, *16*. [[CrossRef](#)]
25. Gupta, S.M.; Tripathi, M. A review of TiO<sub>2</sub> nanoparticles. *Chin. Sci. Bull.* **2011**, *56*, 1639–1657. [[CrossRef](#)]
26. Ghosh, S.; Das, A.P. Modified titanium oxide (TiO<sub>2</sub>) nanocomposites and its array of applications: A review. *Toxicol. Environ. Chem.* **2015**, 97. [[CrossRef](#)]
27. Fua, J.; Wanga, X.; Mac, Z.; Wenmingd, H.; Lie, J.; Wanga, Z.; Wanga, L. Photocatalytic ultrafiltration membranes based on visible light responsive photocatalyst: A review. *Desalin. Water Treat.* **2019**, 168. [[CrossRef](#)]
28. Sabzehmeidani, M.M.; Ghaedi, M.; Karimi, H. Photocatalytic activity based on electrospun nanofibers. In *Interface Science and Technology*; Elsevier: Amsterdam, The Netherlands, 2021; Volume 32, pp. 625–672.
29. Umar, M.; Aziz, H.A. Photocatalytic degradation of organic pollutants in water. Organic pollutants-monitoring, risk and treatment. *Org. Pollut.-Monit. Risk Treat.* **2013**, *30*, 196–197.
30. Padmanabhan, N.T.; John, H. Titanium dioxide based self-cleaning smart surfaces: A short review. *J. Environ. Chem. Eng.* **2020**, *8*. [[CrossRef](#)]
31. Jhaveri, J.H.; Murthy, Z.V.P. A comprehensive review on anti-fouling nanocomposite membranes for pressure driven membrane separation processes. *Desalination* **2016**, 379. [[CrossRef](#)]

32. Ola, O.; Maroto-Valer, M.M. Review of material design and reactor engineering on TiO<sub>2</sub> photocatalysis for CO<sub>2</sub> reduction. *J. Photochem. Photobiol. C Photochem. Rev.* **2015**, *24*. [[CrossRef](#)]
33. Brunetti, A.; Pomilla, F.R.; Marci, G.; Garcia-Lopez, E.I.; Fontananova, E.; Palmisano, L.; Barbieri, G. CO<sub>2</sub> reduction by C<sub>3</sub>N<sub>4</sub>-TiO<sub>2</sub> Nafion photocatalytic membrane reactor as a promising environmental pathway to solar fuels. *Appl. Catal. B Environ.* **2019**, *255*. [[CrossRef](#)]
34. Tetteh, E.K.; Ezugbe, E.O.; Rathilal, S.; Asante-Sackey, D. Removal of COD and SO<sub>4</sub> from oil refinery wastewater using a photo-catalytic system-comparing TiO<sub>2</sub> and zeolite efficiencies. *Water* **2020**, *12*, 214. [[CrossRef](#)]
35. Lin, Z.; Li, J.; Shen, W.; Corriou, J.P.; Chen, X.; Xi, H. Different photocatalytic levels of organics in papermaking wastewater by flocculation-photocatalysis and SBR-photocatalysis: Degradation and GC-MS experiments, adsorption and photocatalysis simulations. *Chem. Eng. J.* **2021**, *412*. [[CrossRef](#)]
36. Salmerón, I.; Sharma, P.K.; Polo-López, M.I.; Tolosana, A.; McMichael, S.; Oller, I.; Byrne, J.A.; Fernández-Ibáñez, P. Electrochemically assisted photocatalysis for the simultaneous degradation of organic micro-contaminants and inactivation of microorganisms in water. *Process Saf. Environ. Prot.* **2021**, *147*. [[CrossRef](#)]
37. Dominguez, S.; Huebra, M.; Han, C.; Campo, P.; Nadagouda, M.N.; Rivero, M.J.; Ortiz, I.; Dionysiou, D.D. Magnetically recoverable TiO<sub>2</sub>-WO<sub>3</sub> photocatalyst to oxidize bisphenol A from model wastewater under simulated solar light. *Environ. Sci. Pollut. Res.* **2017**, *24*, 12589–12598. [[CrossRef](#)] [[PubMed](#)]
38. Otieno, O.V.; Csáki, E.; Kéri, O.; Simon, L.; Lukács, I.E.; Szécsényi, K.M.; Szilágyi, I.M. Synthesis of TiO<sub>2</sub> nanofibers by electrospinning using water-soluble Ti-precursor. *J. Therm. Anal. Calorim.* **2020**, *139*. [[CrossRef](#)]
39. Chen, F.; Zhao, J. Preparation and photocatalytic properties of a novel kind of loaded photocatalyst of TiO<sub>2</sub>/SiO<sub>2</sub>/γ-Fe<sub>2</sub>O<sub>3</sub>. *Catal. Letters* **1999**, *58*. [[CrossRef](#)]
40. Faraldos, M.; Bahamonde, A. Environmental applications of titania-graphene photocatalysts. *Catal. Today* **2017**, *285*. [[CrossRef](#)]
41. Esfandiari, N.; Kashefi, M.; Afsharnejhad, S.; Mirjalili, M. Insight into enhanced visible light photocatalytic activity of Fe<sub>3</sub>O<sub>4</sub>-SiO<sub>2</sub>-TiO<sub>2</sub> core-multishell nanoparticles on the elimination of Escherichia coli. *Mater. Chem. Phys.* **2020**, *244*. [[CrossRef](#)]
42. Li, Q.; Kong, H.; Li, P.; Shao, J.; He, Y. Photo-Fenton degradation of amoxicillin via magnetic TiO<sub>2</sub>-graphene oxide-Fe<sub>3</sub>O<sub>4</sub> composite with a submerged magnetic separation membrane photocatalytic reactor (SMSMPR). *J. Hazard. Mater.* **2019**, *373*. [[CrossRef](#)]
43. Sun, T.; Liu, Y.; Shen, L.; Xu, Y.; Li, R.; Huang, L.; Lin, H. Magnetic field assisted arrangement of photocatalytic TiO<sub>2</sub> particles on membrane surface to enhance membrane antifouling performance for water treatment. *J. Colloid Interface Sci.* **2020**, *570*. [[CrossRef](#)]
44. Zhao, T.; Qian, R.; Zhou, G.; Wang, Y.; Lee, W.I.; Pan, J.H. Mesoporous WO<sub>3</sub>/TiO<sub>2</sub> spheres with tailored surface properties for concurrent solar photocatalysis and membrane filtration. *Chemosphere* **2021**, *263*. [[CrossRef](#)]
45. Nasrollahi, N.; Ghalamchi, L.; Vatanpour, V.; Khataee, A. Photocatalytic-membrane technology: A critical review for membrane fouling mitigation. *J. Ind. Eng. Chem.* **2021**, *93*. [[CrossRef](#)]
46. Maroudas, A.; Pandis, P.K.; Chatzopoulou, A.; Davellas, L.R.; Sourkouni, G.; Argirusis, C. Synergetic decolorization of azo dyes using ultrasounds, photocatalysis and photo-fenton reaction. *Ultrason. Sonochem.* **2021**, *71*. [[CrossRef](#)]
47. Ge, M.; Li, Q.; Cao, C.; Huang, J.; Li, S.; Zhang, S.; Chen, Z.; Zhang, K.; Al-Deyab, S.S.; Lai, Y. One-dimensional TiO<sub>2</sub> Nanotube Photocatalysts for Solar Water Splitting. *Adv. Sci.* **2017**, *4*. [[CrossRef](#)]
48. Kuvarega, A.T.; Mamba, B.B. Photocatalytic Membranes for Efficient Water Treatment. In *Semiconductor Photocatalysis Materials, Mechanisms and Applications*; IntechOpen: London, UK, 2016.
49. di Paola, A.; Bellardita, M.; Palmisano, L. Brookite the least known TiO<sub>2</sub> photocatalyst. *Catalysts* **2013**, *3*, 36. [[CrossRef](#)]
50. Shayegan, Z.; Lee, C.S.; Haghghat, F. TiO<sub>2</sub> photocatalyst for removal of volatile organic compounds in gas phase—A review. *Chem. Eng. J.* **2018**, *334*. [[CrossRef](#)]
51. Naldoni, A.; Altomare, M.; Zoppellaro, G.; Liu, N.; Kment, S.; Zbořil, R.; Schmuki, P. Photocatalysis with reduced TiO<sub>2</sub>: From Black TiO<sub>2</sub> to cocatalyst-free hydrogen production. *ACS Catal.* **2019**, *9*, 345–364. [[CrossRef](#)]
52. Vaiano, V.; Sacco, O.; Sannino, D.; Stoller, M.; Ciambelli, P.; Chianese, A. Photocatalytic removal of phenol by ferromagnetic N-TiO<sub>2</sub>/SiO<sub>2</sub>/Fe<sub>3</sub>O<sub>4</sub> nanoparticles in presence of visible light irradiation. *Chem. Eng. Trans.* **2016**, *47*, 235–240. [[CrossRef](#)]
53. Abdullah, H.; Khan, M.M.R.; Ong, H.R.; Yaakob, Z. Modified TiO<sub>2</sub> photocatalyst for CO<sub>2</sub> photocatalytic reduction: An overview. *J. CO<sub>2</sub> Util.* **2017**, *22*. [[CrossRef](#)]
54. Bhanvase, B.A.; Shende, T.P.; Sonawane, S.H. A review on graphene-TiO<sub>2</sub> and doped graphene-TiO<sub>2</sub> nanocomposite photocatalyst for water and wastewater treatment. *Environ. Technol. Rev.* **2017**, *6*. [[CrossRef](#)]
55. Lee, S.Y.; Park, S.J. TiO<sub>2</sub> photocatalyst for water treatment applications. *J. Ind. Eng. Chem.* **2013**, *19*. [[CrossRef](#)]
56. Sharma, A.; Liu, N.; Ma, Q.; Zheng, H.; Kawazoe, N.; Chen, G.; Yang, Y. PEG assisted P/Ag/Ag<sub>2</sub>O/Ag<sub>3</sub>PO<sub>4</sub>/TiO<sub>2</sub> photocatalyst with enhanced elimination of emerging organic pollutants in salinity condition under solar light illumination. *Chem. Eng. J.* **2020**, *385*. [[CrossRef](#)]
57. Izadpanah, M.; Sarrafzadeh, M.H.; Rezaei-Dashtarzhandi, M.; Vojoudi, H. Aquatic center sewage reclamation and water reuse, using an integrated system combining adsorption, RO membrane system, and TiO<sub>2</sub>/Fe<sub>3</sub>O<sub>4</sub> photocatalytic oxidation. *J. Environ. Chem. Eng.* **2021**, *9*. [[CrossRef](#)]
58. Zhang, R.; Ma, Y.; Lan, W.; Sameen, D.E.; Ahmed, S.; Dai, J.; Qin, W.; Li, S.; Liu, Y. Enhanced photocatalytic degradation of organic dyes by ultrasonic-assisted electrospray TiO<sub>2</sub>/graphene oxide on polyacrylonitrile/β-cyclodextrin nanofibrous membranes. *Ultrason. Sonochem.* **2021**, *70*. [[CrossRef](#)]

59. Lakshmanan, R. Application of Magnetic Nanoparticles and Reactive Filter Materials for Wastewater Treatment Ramnath Lakshmanan. Ph.D. Thesis, KTH Royal Institute of Technology, Stockholm, Sweden, 2013.
60. Ahangar, L.E.; Movassaghi, K.; Emadi, M.; Yaghoobi, F. Photocatalytic application of TiO<sub>2</sub> / SiO<sub>2</sub>-based magnetic nanocomposite (Fe<sub>3</sub>O<sub>4</sub> @ SiO<sub>2</sub> / TiO<sub>2</sub>) for reusing of textile wastewater. *Nano Chem. Res.* **2016**, *1*, 33–39. [[CrossRef](#)]
61. Ma, L.; Chen, Y.; Zheng, J. An efficient, stable and reusable polymer/TiO<sub>2</sub> photocatalytic membrane for aqueous pollution treatment. *J. Mater. Sci.* **2021**. [[CrossRef](#)]
62. Liu, N.; Schneider, C.; Freitag, D.; Venkatesan, U.; Marthala, V.R.; Hartmann, M.; Winter, B.; Spiecker, E.; Osvet, A.; Zolnhofer, E.M.; et al. Hydrogenated anatase: Strong photocatalytic dihydrogen evolution without the use of a co-catalyst. *Angew. Chemie Int. Ed.* **2014**, *53*, 14201–14205. [[CrossRef](#)]
63. Xu, X.; Liu, S.; Smith, K.; Wang, Y.; Hu, H. Light-driven breakdown of 1,4-Dioxane for potable reuse: A review. *Chem. Eng. J.* **2019**, *373*. [[CrossRef](#)]
64. Pirilä, M. *Adsorption and Photocatalysis in Water Treatment: Active, Abundant and Inexpensive Materials and Methods*; Acta Universitatis Ouluensis, University of Oulu: Oulu, Finland, 2015.
65. Barakat, N.A.M.; Erfan, N.A.; Mohammed, A.A.; Mohamed, S.E.I. Ag-decorated TiO<sub>2</sub> nanofibers as Arrhenius equation-incompatible and effective photocatalyst for water splitting under visible light irradiation. *Colloids Surf. A Physicochem. Eng. Asp.* **2020**, *604*. [[CrossRef](#)]
66. Nguyen-Phan, T.D.; Luo, S.; Liu, Z.; Gamalski, A.D.; Tao, J.; Xu, W.; Stach, E.A.; Polyansky, D.E.; Senanayake, S.D.; Fujita, E.; et al. Striving Toward Noble-Metal-Free Photocatalytic Water Splitting: The Hydrogenated-Graphene – TiO<sub>2</sub> Prototype. *Chem. Mater.* **2015**, *27*, 6282–6296. [[CrossRef](#)]
67. Chen, F.; Xie, Y.; Zhao, J.; Lu, G. Photocatalytic degradation of dyes on a magnetically separated photocatalyst under visible and UV irradiation. *Chemosphere* **2001**, *44*. [[CrossRef](#)]
68. Zhang, A.-P.; Sun, Y.-P. Photocatalytic killing effect of Fe<sub>3</sub>O<sub>4</sub>-TiO<sub>2</sub>nanoparticles on hepatoma carcinoma cells for targeting photodynamic therapy. *Chinese J. Inorg. Chem.* **2017**, *32*. [[CrossRef](#)]
69. Sakarkar, S.; Muthukumran, S.; Jegatheesan, V. Factors affecting the degradation of remazol turquoise blue (RTB) dye by titanium dioxide (TiO<sub>2</sub>) entrapped photocatalytic membrane. *J. Environ. Manag.* **2020**, *272*. [[CrossRef](#)]
70. Tetteh, E.K.; Rathilal, S. Kinetics and nanoparticle catalytic enhancement of biogas production from wastewater using a magnetized biochemical methane potential (Mbmp) system. *Catalysts* **2020**, *10*, 1200. [[CrossRef](#)]
71. Blanco, M.; Monteserín, C.; Angulo, A.; Pérez-Márquez, A.; Maudes, J.; Murillo, N.; Aranzabe, E.; Ruiz-Rubio, L.; Vilas, J.L. TiO<sub>2</sub>-doped electrospun nanofibrous membrane for photocatalytic water treatment. *Polymers* **2019**, *11*, 747. [[CrossRef](#)]
72. Ghernaout, D. Magnetic field generation in the water treatment perspectives: An overview. *Int. J. Adv. Appl. Sci.* **2017**, *5*, 193–203. [[CrossRef](#)]
73. Štefušová, K.; Václavíková, M.; Lovás, M.; Hredzák, S. Use of magnetic filtration in wastewater treatment. *Acta Montan. Slovaca* **2012**, *17*, 81–84.
74. Yao, H.; Fan, M.; Wang, Y.; Luo, G.; Fei, W. Magnetic titanium dioxide-based nanomaterials: Synthesis, characteristics, and photocatalytic application in pollutant degradation. *J. Mater. Chem. A* **2015**, *3*, 17511–17524. [[CrossRef](#)]
75. Marinko, Ž.; Suhadolnik, L.; Samardžija, Z.; Kovač, J.; Čeh, M. The influence of a surface treatment of metallic titanium on the photocatalytic properties of TiO<sub>2</sub> nanotubes grown by anodic oxidation. *Catalysts* **2020**, *10*, 803. [[CrossRef](#)]
76. Tetteh, E.K.; Naidoo, D.B.; Rathilal, S. Optimization of photo-catalytic degradation of oil refinery wastewater using Box-Behnken design. *Environ. Eng. Res.* **2019**, *24*. [[CrossRef](#)]
77. Heng, J.Z.X.; Tang, K.Y.; Regulacio, M.D.; Lin, M.; Loh, X.J.; Li, Z.; Ye, E. Solar-powered photodegradation of pollutant dyes using silver-embedded porous TiO<sub>2</sub> nanofibers. *Nanomaterials* **2021**, *11*, 856. [[CrossRef](#)]
78. Sharotri, N.; Sharma, D.; Sud, D. Experimental and theoretical investigations of Mn-N-co-doped TiO<sub>2</sub> photocatalyst for visible light induced degradation of organic pollutants. *J. Mater. Res. Technol.* **2019**, *8*. [[CrossRef](#)]
79. Liu, H.; Dao, A.Q.; Fu, C. Activities of combined TiO<sub>2</sub> semiconductor nanocatalysts under solar light on the reduction of CO<sub>2</sub>. *J. Nanosci. Nanotechnol.* **2016**, *16*. [[CrossRef](#)]
80. Wu, J.C.S.; Huang, C.W. In situ DRIFTS study of photocatalytic CO<sub>2</sub> reduction under UV irradiation. *Front. Chem. Eng. China* **2010**, *4*, 120–126. [[CrossRef](#)]
81. Goei, R.; Lim, T.T. Ag-decorated TiO<sub>2</sub> photocatalytic membrane with hierarchical architecture: Photocatalytic and anti-bacterial activities. *Water Res.* **2014**, *59*. [[CrossRef](#)]
82. Liu, X.; Wang, L.; Zhou, X.; He, X.; Zhou, M.; Jia, K.; Liu, X. Design of polymer composite-based porous membrane for in-situ photocatalytic degradation of adsorbed organic dyes. *J. Phys. Chem. Solids* **2021**, *154*. [[CrossRef](#)]
83. Jia, Y.; Cai, F.; Lu, S.; Yang, F.; Zhao, Y. Research on the preparation and application of through-hole TiO<sub>2</sub> nanotube arrays membranes. *Cailiao Daobao/Materials Rev.* **2016**, *30*. [[CrossRef](#)]
84. Chong, M.N.; Jin, B.; Chow, C.W.K.; Saint, C. Recent developments in photocatalytic water treatment technology: A review. *Water Res.* **2010**, *44*. [[CrossRef](#)]
85. Penboon, L.; Khruakham, A.; Sairiam, S. TiO<sub>2</sub> coated on PVDF membrane for dye wastewater treatment by a photocatalytic membrane. *Water Sci. Technol.* **2019**, *79*. [[CrossRef](#)]

86. Bergamasco, R.; Coldebella, P.F.; Camacho, F.P.; Rezende, D.; Yamaguchi, N.U.; Klen, M.R.F.; Tavares, C.J.M.; Amorim, M.T.S.P. Self-assembly modification of polyamide membrane by coating titanium dioxide nanoparticles for water treatment applications. *Rev. Ambient. E Agua* **2019**, *14*. [[CrossRef](#)]
87. Kacprzyńska-Gońska, J.; Łożyńska, M.; Barszcz, W.; Sowa, S.; Wiciński, P.; Woskowicz, E. Microfiltration membranes modified with composition of titanium oxide and silver oxide by magnetron sputtering. *Polymers* **2021**, *13*, 141. [[CrossRef](#)]
88. Ou, W.; Pan, J.; Liu, Y.; Li, S.; Li, H.; Zhao, W.; Wang, J.; Song, C.; Zheng, Y.; Li, C. Two-dimensional ultrathin MoS<sub>2</sub>-modified black Ti<sup>3+</sup>-TiO<sub>2</sub> nanotubes for enhanced photocatalytic water splitting hydrogen production. *J. Energy Chem.* **2020**, *43*. [[CrossRef](#)]
89. Wang, R.; Shi, M.; Xu, F.; Qiu, Y.; Zhang, P.; Shen, K.; Zhao, Q.; Yu, J.; Zhang, Y. Graphdiyne-modified TiO<sub>2</sub> nanofibers with osteoinductive and enhanced photocatalytic antibacterial activities to prevent implant infection. *Nat. Commun.* **2020**, *11*. [[CrossRef](#)]
90. Zhang, Q.; Song, Y.; Guo, J.; Wu, S.; Chen, N.; Fan, H.; Gao, M.; Yang, J.; Sheng, Z.; Lang, J. One-step hydrothermal synthesis of the modified carbon cloth membrane: Towards visible light driven and self-cleaning for efficient oil-water separation. *Surf. Coatings Technol.* **2021**, *409*. [[CrossRef](#)]
91. Arifin, K.; Yunus, R.M.; Minggu, L.J.; Kassim, M.B. Improvement of TiO<sub>2</sub> nanotubes for photoelectrochemical water splitting: Review. *Int. J. Hydrogen Energy* **2021**, *46*. [[CrossRef](#)]
92. Fu, F.; Cha, G.; Denisov, N.; Chen, Y.; Zhang, Y.; Schmuki, P. Water Annealing of TiO<sub>2</sub> Nanotubes for Photocatalysis Revisited. *ChemElectroChem* **2020**, *7*. [[CrossRef](#)]
93. Mansouri, S.; Abbaspour-Fard, M.H.; Meshkini, A. Lily (Iris Persica) pigments as new sensitizer and TiO<sub>2</sub> nanofibers as photoanode electrode in dye sensitized solar cells. *Optik* **2020**, *202*. [[CrossRef](#)]
94. Gao, J.; Jia, S.; Liu, J.; Sun, Z.; Yang, X.; Tang, D. Enhanced effect of adsorption and photocatalysis by TiO<sub>2</sub> nanoparticles embedded porous PVDF nanofiber scaffolds. *J. Mater. Res.* **2021**. [[CrossRef](#)]
95. Song, J.; Wang, X.; Yan, J.; Yu, J.; Sun, G.; Ding, B. Soft Zr-doped TiO<sub>2</sub> Nanofibrous Membranes with Enhanced Photocatalytic Activity for Water Purification. *Sci. Rep.* **2017**, *7*. [[CrossRef](#)]
96. Joseph, E.; Madhusudan, S.P.; Mohanta, K.; Karthega, M.; Batabyal, S.K. Multiple negative differential resistance in perovskite (CH<sub>3</sub>NH<sub>3</sub>PbI<sub>3</sub>) decorated electrospun TiO<sub>2</sub> nanofibers. *Appl. Phys. A Mater. Sci. Process.* **2020**, *126*. [[CrossRef](#)]
97. Abdelmaksoud, M.; Mohamed, A.; Sayed, A.; Khairy, S. Physical properties of PVDF-GO/black-TiO<sub>2</sub> nanofibers and its photocatalytic degradation of methylene blue and malachite green dyes. *Environ. Sci. Pollut. Res.* **2021**. [[CrossRef](#)]
98. Dong, M.; Li, Q.H.; Li, R.; Cui, Y.Q.; Wang, X.X.; Yu, J.Q.; Long, Y.Z. Efficient under visible catalysts from electrospun flexible Ag<sub>2</sub>S/TiO<sub>2</sub> composite fiber membrane. *J. Mater. Sci.* **2021**, *56*. [[CrossRef](#)]
99. Huang, G.; Liu, X.; Shi, S.; Li, S.; Xiao, Z.; Zhen, W.; Liu, S.; Wong, P. Hydrogen producing water treatment through mesoporous TiO<sub>2</sub> nanofibers with oriented nanocrystals. *Chinese J. Catal.* **2020**, *41*. [[CrossRef](#)]
100. Liu, L.; Liu, Z.; Bai, H.; Sun, D.D. Concurrent filtration and solar photocatalytic disinfection/degradation using high-performance Ag/TiO<sub>2</sub> nanofiber membrane. *Water Res.* **2012**, *46*. [[CrossRef](#)]
101. Al-Hajji, L.A.; Ismail, A.A.; Alsaidi, M.; Ahmed, S.A.; Almutawa, F.; Bumajdad, A. Comparison of TiO<sub>2</sub> nanowires and TiO<sub>2</sub> nanoparticles for photodegradation of resorcinol as endocrine model. *J. Nanoparticle Res.* **2020**, *22*. [[CrossRef](#)]
102. Zhang, X.; Du, A.J.; Lee, P.; Sun, D.D.; Leckie, J.O. TiO<sub>2</sub> nanowire membrane for concurrent filtration and photocatalytic oxidation of humic acid in water. *J. Memb. Sci.* **2008**, *313*, 44–51. [[CrossRef](#)]
103. Wang, G.; Wang, H.; Ling, Y.; Tang, Y.; Yang, X.; Fitzmorris, R.C.; Wang, C.; Zhang, J.Z.; Li, Y. Hydrogen-treated TiO<sub>2</sub> nanowire arrays for photoelectrochemical water splitting. *Nano Lett.* **2011**, *11*. [[CrossRef](#)]
104. Qi, H.; Wu, Y. Synaptic plasticity of TiO<sub>2</sub> nanowire transistor. *Microelectron. Int.* **2020**, *37*. [[CrossRef](#)]
105. Koseoglu-Imer, D.Y.; Koyuncu, I. Fabrication and application areas of mixed matrix flat-sheet membranes. In *Application of Nanotechnology in Membranes for Water Treatment*; CRC Press: Boca Raton, FL, USA, 2017; pp. 49–66.
106. Yang, C.; Wang, P.; Li, J.; Wang, Q.; Xu, P.; You, S.; Zheng, Q.; Zhang, G. Photocatalytic PVDF ultrafiltration membrane blended with visible-light responsive Fe (III)-TiO<sub>2</sub> catalyst: Degradation kinetics, catalytic performance and reusability. *Chem. Eng. J.* **2021**, *417*. [[CrossRef](#)]
107. Sakarkar, S.; Muthukumar, S.; Jegatheesan, V. Tailoring the effects of titanium dioxide (TiO<sub>2</sub>) and polyvinyl alcohol (pva) in the separation and antifouling performance of thin-film composite polyvinylidene fluoride (pvdf) membrane. *Membranes* **2021**, *11*, 241. [[CrossRef](#)]
108. Hamed, S.M.; Abdollah, F.S.; Nosratollah, M. Preparation, characterization, and performance study of PVDF nanocomposite contained hybrid nanostructure TiO<sub>2</sub>-POM used as a photocatalytic membrane. *Iran. J. Chem. Chem. Eng.* **2021**, *40*. [[CrossRef](#)]
109. Choi, H.; Antoniou, M.G.; de la Cruz, A.A.; Stathatos, E.; Dionysiou, D.D. Photocatalytic TiO<sub>2</sub> films and membranes for the development of efficient wastewater treatment and reuse systems. *Desalination* **2007**, *202*, 199–206. [[CrossRef](#)]
110. Corredor, J.; Perez-Peña, E.; Rivero, M.J.; Ortiz, I. Performance of rgo/tio<sub>2</sub> photocatalytic membranes for hydrogen production. *Membranes* **2020**, *10*, 218. [[CrossRef](#)]
111. Yan, M.; Wu, Y.; Liu, X. Photocatalytic nanocomposite membranes for high-efficiency degradation of tetracycline under visible light: An imitated core-shell Au-TiO<sub>2</sub>-based design. *J. Alloys Compd.* **2021**, *855*. [[CrossRef](#)]
112. Sun, J.; Li, S.; Ran, Z.; Xiang, Y. Preparation of Fe<sub>3</sub>O<sub>4</sub>@TiO<sub>2</sub> blended PVDF membrane by magnetic coagulation bath and its permeability and pollution resistance. *J. Mater. Res. Technol.* **2020**. [[CrossRef](#)]
113. Heng, Z.W.; Chong, W.C.; Pang, Y.L.; Sim, L.C.; Koo, C.H. Novel visible-light responsive NCQDs-TiO<sub>2</sub>/PAA/PES photocatalytic membrane with enhanced antifouling properties and self-cleaning performance. *J. Environ. Chem. Eng.* **2021**, *9*. [[CrossRef](#)]

114. Wang, Y.; Dai, L.; Qu, K.; Qin, L.; Zhuang, L.; Yang, H.; Xu, Z. Novel Ag-AgBr decorated composite membrane for dye rejection and photodegradation under visible light. *Front. Chem. Sci. Eng.* **2021**. [[CrossRef](#)]
115. Goei, R.; Dong, Z.; Lim, T.T. High-permeability pluronic-based TiO<sub>2</sub> hybrid photocatalytic membrane with hierarchical porosity: Fabrication, characterizations and performances. *Chem. Eng. J.* **2013**, *228*. [[CrossRef](#)]
116. Wang, L. Configurations and Membranes of Photocatalytic Membrane Reactors for Water and Wastewater Treatment. In *IOP Conference Series: Earth and Environmental Science*; IOP Publishing: Hong Kong, China, 2018; Volume 208. [[CrossRef](#)]
117. Riaz, S.; Park, S.J. An overview of TiO<sub>2</sub>-based photocatalytic membrane reactors for water and wastewater treatments. *J. Ind. Eng. Chem.* **2020**, *84*. [[CrossRef](#)]
118. Zangeneh, H.; Zinatizadeh, A.A.; Zinadini, S.; Feyzi, M.; Bahnemann, D.W. Preparation and characterization of a novel photocatalytic self-cleaning PES nanofiltration membrane by embedding a visible-driven photocatalyst boron doped-TiO<sub>2</sub>-SiO<sub>2</sub>/CoFe<sub>2</sub>O<sub>4</sub> nanoparticles. *Sep. Purif. Technol.* **2019**, *209*. [[CrossRef](#)]
119. Horovitz, I.; Avisar, D.; Baker, M.A.; Grilli, R.; Lozzi, L.; Di Camillo, D.; Mamane, H. Carbamazepine degradation using a N-doped TiO<sub>2</sub> coated photocatalytic membrane reactor: Influence of physical parameters. *J. Hazard. Mater.* **2016**, *310*. [[CrossRef](#)] [[PubMed](#)]
120. Symes, D.; Taylor-Cox, C.; Holyfield, L.; Al-Duri, B.; Dhir, A. Feasibility of an oxygen-getter with nickel electrodes in alkaline electrolyzers. *Mater. Renew. Sustain. Energy* **2014**, *3*. [[CrossRef](#)]
121. Zhang, Y.; Li, Q.; Gao, Q.; Wan, S.; Yao, P.; Zhu, X. Preparation of Ag/ $\beta$ -cyclodextrin co-doped TiO<sub>2</sub> floating photocatalytic membrane for dynamic adsorption and photoactivity under visible light. *Appl. Catal. B Environ.* **2020**, *267*. [[CrossRef](#)]
122. Kang, Y.; Jiao, S.; Zhao, Y.; Wang, B.; Zhang, Z.; Yin, W.; Tan, Y.; Pang, G. High-flux and high rejection TiO<sub>2</sub> nanofibers ultrafiltration membrane with porous titanium as supporter. *Sep. Purif. Technol.* **2020**, *248*. [[CrossRef](#)]
123. Baniamer, M.; Aroujalian, A.; Sharifnia, S. Photocatalytic membrane reactor for simultaneous separation and photoreduction of CO<sub>2</sub> to methanol. *Int. J. Energy Res.* **2021**, *45*. [[CrossRef](#)]
124. Baskar, D.; Nallathambi, G.; Selvam, A.K.; Kumar, P.S. Preparation of pan/lycopene-tio<sub>2</sub> nanocomposite membrane for azo dye degradation. *Desalin. Water Treat.* **2021**, *216*. [[CrossRef](#)]
125. Wafiroh, S.; Wibiarisky, A.M. Abdulloh Application of cellulose acetate-TiO<sub>2</sub> hollow fiber photocatalytic membrane composite for profenofos degradation. *Pollut. Res.* **2019**, *38*, S183–S189.
126. Manouras, T.; Koufakis, E.; Vasilaki, E.; Peraki, I.; Vamvakaki, M. Antimicrobial Hybrid Coatings Combining Enhanced Biocidal Activity under Visible-Light Irradiation with Stimuli-Renewable Properties. *ACS Appl. Mater. Interfaces* **2021**. [[CrossRef](#)]
127. Nemet, A.; Varbanov, P.S.; Klemeš, J.J. Erratum to: Cleaner production, Process Integration and intensification (Clean Techn Environ Policy, 10.1007/s10098-016-1240-x). *Clean Technol. Environ. Policy* **2016**, *18*. [[CrossRef](#)]
128. Zhang, M.; Huang, Q.; Huang, Y.; Xiao, C. Electrospun poly(tetrafluoroethylene)/TiO<sub>2</sub> photocatalytic nanofiber membrane and its application. *Fangzhi Xuebao/Journal Text. Res.* **2019**, *40*. [[CrossRef](#)]
129. Zhang, X.; Wang, D.K.; Lopez, D.R.S.; da Costa, J.C.D. Fabrication of nanostructured TiO<sub>2</sub> hollow fiber photocatalytic membrane and application for wastewater treatment. *Chem. Eng. J.* **2014**, *236*. [[CrossRef](#)]
130. Li, J.; Li, B.; Sui, G.; Du, L.; Zhuang, Y.; Zhang, Y.; Zou, Y. Removal of volatile organic compounds from air using supported ionic liquid membrane containing ultraviolet-visible light-driven Nd-TiO<sub>2</sub> nanoparticles. *J. Mol. Struct.* **2021**, *1231*. [[CrossRef](#)]
131. Shetty, R.; Chavan, V.B.; Kulkarni, P.S.; Kulkarni, B.D.; Kamble, S.P. Photocatalytic Degradation of Pharmaceuticals Pollutants Using N-Doped TiO<sub>2</sub> Photocatalyst: Identification of CFX Degradation Intermediates. *Indian Chem. Eng.* **2017**, *59*. [[CrossRef](#)]
132. Mohammad, N.; Atassi, Y. TiO<sub>2</sub>/PLLA Electrospun Nanofibers Membranes for Efficient Removal of Methylene Blue Using Sunlight. *J. Polym. Environ.* **2021**, *29*. [[CrossRef](#)]
133. Mpelane, A.; Katwire, D.M.; Mungondori, H.H.; Nyamukamba, P.; Taziwa, R.T. Application of novel c-tio<sub>2</sub>-cfa/pan photocatalytic membranes in the removal of textile dyes in wastewater. *Catalysts* **2020**, *10*, 909. [[CrossRef](#)]
134. Paredes, L.; Murgolo, S.; Dzinun, H.; Othman, M.H.D.; Ismail, A.F.; Carballa, M.; Mascolo, G. Application of immobilized TiO<sub>2</sub> on PVDF dual layer hollow fibre membrane to improve the photocatalytic removal of pharmaceuticals in different water matrices. *Appl. Catal. B Environ.* **2019**, *240*. [[CrossRef](#)]